HOW MUCH IRON IS GOOD? REVISITING THE ROLE OF FERROUS IRON SUPPLEMENTATION IN CULTURED CELLS USING GENETICALLY ENCODED NO BIOSENSORS

by
GÜLŞAH SEVİMLİ

Submitted to the Graduate School of Engineering and Natural Sciences
in partial fulfillment of
the requirements for the degree of Master of Science

Sabancı University
December 2021

HOW MUCH IRON IS GOOD? REVISITING THE ROLE OF FERROUS IRON SUPPLEMENTATION IN CULTURED CELLS USING GENETICALLY ENCODED NO BIOSENSORS

APPROVED BY:

DATE OF APPROVAL: December 17, 2021

ABSTRACT

HOW MUCH IRON IS GOOD? REVISITING THE ROLE OF FERROUS IRON SUPPLEMENTATION IN CULTURED CELLS USING GENETICALLY ENCODED NO BIOSENSORS

GÜLŞAH SEVİMLİ

Molecular Biology, Genetics and Bioengineering, MSc. Thesis, December 2021

Thesis Supervisor: Prof. Dr. Levent Öztürk

Thesis Co-Supervisor: Dr. Emrah Eroğlu

Keywords: cell culture media, ferrous iron (Fe^{2+}), genetically encoded NO probes (geNOps), vitamin C

Although ferrous iron (Fe^{2+}) is an essential cofactor for many metalloproteins, most cell culture media lack or only contain insufficient amounts of this transient metal, resulting in iron (II) deficiency in cultured cells. Well-established techniques permit quantification of Fe^{2+} in cells with high accuracy; however, these techniques do not provide information about the iron-dependent functionality of metalloprotein. In this study, we demonstrated that genetically encoded nitric oxide probe (geNOps), which comprises a non-heme iron-binding protein (GAF) fused with a fluorescent protein, can be utilized as an indirect model system to study the iron-dependency in cultured cells. In the presence of NO, the GAF domain can be reversibly nitrosylated causing changes in the fluorescence intensity in a concentration-dependent manner. We showed that long-term supplementation of Fe^{2+} in cultured cells has no effect on the functionality of geNOps. Only short-term provision of freshly prepared Fe^{2+} combined with vitamin C activated the metalloprotein. The distribution of Fe^{2+} in cells after short-term treatment was observed with the FeRhoNox-1 and the accumulation of total iron was determined using high-resolution light microscopy techniques and Perls/DAB staining. Employing the design of experiment approaches, we optimized the Fe^{2+} loading procedure regarding Fe^{2+} and vitamin C concentrations and the duration of cell treatment. This approach yielded a non-toxic Fe^{2+} supplementation procedure that is essential for cell integrity and the full functionality of metalloprotein. In conclusion, this study exploited a metalloprotein readout to extrapolate the Fe^{2+} uptake capability of cells under cell culture conditions.

ÖZET

NE KADAR DEMİR İYİDİR? GENETİK KODLANMIŞ NO PROBLARI KULLANARAK KÜLTÜRLENMİŞ HÜCRELERDE FERRÖZ DEMİR TAKVİYESİNİN ROLÜNÜN İNCELENMESİ

GÜLŞAH SEVİMLİ

Moleküler Biyoloji, Genetik ve Biyomühendislik, Yüksek Lisans Tezi, Aralık 2021

Tez Danışmanı: Prof. Dr. Levent Öztürk

Tez Eş-Danışmanı: Dr. Emrah Eroğlu

Anahtar Kelimeler: ferröz demir (Fe^{2+}), genetik kodlanmış NO probları (geNOps), hücre kültürü besiyeri, vitamin C

Ferröz demir (Fe^{2+}) birçok metalloprotein için temel bir kofaktör olmasına rağmen, çoğu hücre kültürü besiyeri bu geçici metalden yoksundur veya yetersiz miktarda içermektedir, bu da kültürlenmiş hücrelerde demir (II) eksikliğine neden olmaktadır. Yüksek hassasiyete sahip teknikler, hücrelerde Fe^{2+} miktarının belirlenmesine izin vermektedir, ancak bu teknikler metalloproteinin demire bağımlı işlevselliği hakkında bilgi sağlamamaktadır. Bu çalışmada, bir floresan protein ile kaynaştırılmış, hem olmayan demir bağlayıcı bir protein (GAF) içeren genetik kodlanmış nitrik oksit probunun (geNOps) kültürlenmiş hücrelerde demir bağımlılığını incelemek için dolaylı bir model sistem olarak kullanılabileceğini gösterdik. NO varlığında, GAF alanında konsantrasyona bağlı oluşan nitrosillenme floresan yoğunluğunda değişikliğe sebep olmaktadır. Kültürlenmiş hücrelerde uzun süreli Fe^{2+} takviyesinin geNOps'un işlevselliği üzerinde hiçbir etkisi olmadığını gösterdik. Sadece kısa süreli taze hazırlanmış Fe^{2+} ve C vitamini metalloproteini aktive etti. Kısa süreli Fe^{2+} takviyesi sonrası hücrelerde oluşan demir birikimi, FeRhoNox-1 ile gözlemlendi. Toplam demir ise Perls/DAB boyaması kullanılarak yüksek çözünürlüklü ışık mikroskobu teknikleri ile belirlendi. Deney tasarımı kullanarak Fe^{2+} ve C vitamini konsantrasyonları ve hücre tedavi süresini içeren Fe^{2+} yükleme prosedürünü optimize ettik. Bu yaklaşım, hücre bütünlüğü ve metalloproteinin tam işlevselliği için gerekli olan, toksik olmayan bir Fe^{2+} takviyesi prosedürü sağladı. Sonuç olarak, bu çalışma, hücre kültürü koşulları altında hücrelerin Fe^{2+} alım kapasitesini tahmin etmek için bir metalloprotein okumasından yararlanmıştır.

ACKNOWLEDGEMENTS

I would like to thank Dr. Emrah Eroğlu who has contributed to my MSc education and the achievement of this project. His support, patience, motivation, guidance, sincerity, and vast knowledge have brought my work to such a good point. I am immensely grateful for the academic information he has offered me.

I would like to thank Asal so much for your prime friendship, and the energizing snacks you bring out when we need them most. Büşra, thank you for the advice you gave in times of crisis, for our scientific discussions, and for the fun times we had. I would like to thank Hamza for the advice and effort he gave during my studies. I would like to thank Melike, one of the most beautiful friendships that the laboratory has given me, for all her support. I would also like to thank Tuba for her contribution to my work and for her conversations. I would like to thank Zeynep for the fun moments and conversations we had. I would like to thank Ceyhun, the head of our laboratory in charge of activities, for his support and scientific advice.

Besides, I would like to thank my thesis committee members, Prof. Dr. Levent Öztürk, Asst. Prof. Dr. Nur Mustafaoğlu, Asst. Prof. Dr. Sevde Altuntaş for their inspirational comments and suggestions.

Finally, I am very pleased to have met my former laboratory members, Serap and Emir. I also thank Şükriye Bilir for their efforts and supports in CLEM and confocal experiments.

I would like to thank my lab and dorm neighbour, friend İrem Akülkü for making my time here invaluable and for her support and advice. My special thanks go to 3 excellent friends who have been in my life and have always stood by me and supported me: Kader, Sena, and Tamay. Really thank you for all your support, love, friendship, and put up with me during this time.

Foremost, I would like to express my endless thanks to Özgür Gül, my very esteemed teacher from Istanbul Bilgi University, who formed the basis of my academic career and the science I learned, but who is unfortunately not with us today. I have his momentous contributions to my academic path. I will remember him with great respect and longing for every experiment I do. May his soul rest in peace.

I would like to give special thanks to my great family who raised me and made the greatest contribution to my progress. I am extremely grateful for your prayers, love, care, continuous support, and sacrifices.

In honor of Özgür Gül,
with respect and longing

TABLE OF CONTENTS

LIST OF TABLES

LIST OF FIGURES

LIST OF ABBREVIATIONS

µg	Microgram
µl	Microliter
µM	Micromolar
BF	Bright field
Calcein-AM	Calcein acetoxymethyl ester
CO_2	Carbon dioxide
DAB	3,3'-diaminobenzidine
Dcytb	Duodenal cytochrome b
DMEM	Dulbecco's Modified Eagle Medium
DMT1	Divalent metal transporter 1
EA. hy926	Human umbilical vein cell line
EDTA	Ethylene diamine tetra acetic acid
Fe^{2+}	Ferrous iron
Fe^{3+}	Ferric iron
FBS	Fetal bovine serum
FCS	Fetal calf serum
FP	Fluorescent proteins
GEBs	Genetically encoded biosensors
geNOps	Genetically encoded nitric oxide probes
HCl	Hydrochloric acid
HCP1	Haem carrier protein 1
HEK	Human embryonic kidney
HF	Hydrofluoric acid
HNO_3	Nitric acid
H_2O_2	Hydrogen peroxide
ICP-MS	Inductively coupled plasma mass spectrometry

$KMnO_4$	Potassium permanganate
mM	Millimolar
NO	Nitric oxide
N_2O	Nitrous oxide
OH•	Hydroxyl radical
O_2^-	Superoxide
PI	Propidium iodide
ROS	Reactive oxygen species
TEM	Transmission electron microscopy

1. INTRODUCTION

1.1. Ferrous Iron (Fe^{2+}) Uptake in Cultured Cells

Iron is one of the most important transition metals for all organisms (*Wang & Pantopoulos, 2011*). The presence of reduced iron in cells is necessary for metalloproteins to perform their functions correctly (*Bertini et al., 1995*). Metalloproteins, which are proteins that contain one or more metal ions that act as cofactors in their structure, have important functions such as storage and transport of important signaling molecules within the cell (*Maret, 2010*). Metal ions usually interact with oxygen, sulfur, and nitrogen atoms found in amino acid residues of proteins in metalloproteins (*Hoppert, 2011*). The reactions carried out by the metals in the structure of these proteins are usually reversible (*Hoppert, 2011*). The iron that performs these functions exists in two forms: heme (Fe^{2+}) and non-heme iron (Fe^{3+}) (*Sherman et al., 2018*). Heme iron comes from dietary sources of meat, while non-heme iron comes from plant foods (*Sharp & Sirai, 2007*). Its absorption is higher than non-heme iron since heme iron is more soluble (*Sharp & Sirai, 2007*). The uptake of heme iron is carried out by heme carrier protein 1 (HCP1) in duodenal enterocytes (*Shayeghi et al., 2005*) while the uptake of non-heme iron is provided by the divalent metal transporter 1 (DMT1) (*Waldvogel-Abramowski et al., 2014*). DMT1 passes iron in the ferrous form (Fe^{2+}), therefore non-heme iron

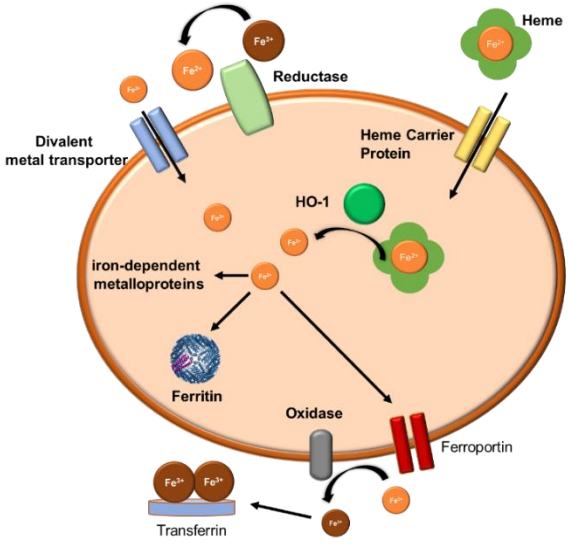

Figure 1.1. Schematic of the iron (II) uptake mechanism.

found in ferric form (Fe^{3+}) is reduced to ferrous iron by reductases such as duodenal cytochrome b (Dcytb) (*Lane et al., 2015*). Vitamin C is also one of the reducing agents that help convert ferric iron into ferrous iron (*Zhitkovich, 2020*). In the presence of Vitamin C, ferric iron is converted to ferrous form by electron transfer that occurs during the conversion of vitamin C to dehydroascorbic acid (*Zhitkovich, 2021*). Then, the absorbed iron is either stored by ferritin or participates in electron transfer reactions or is transported from the cell to the relevant tissues via transferrin (*Waldvogel-Abramowski et al., 2014*).

Ferric iron (Fe^{3+}) binds to transferrin in plasma (*Galaris et al.,2019*). Cells uptake iron by binding iron-bound transfers to transferrin receptors on cell membranes (*Kawabata, 2019*). The expression of transferrin receptors varies with the iron status of the cell (*Galaris et al., 2019*). In iron overload conditions, plasma iron concentration increases and exceeds the iron carrying capacity of transferrin (*Sherman et al., 2018*). In this case, free iron is taken into the cell-by-cell membrane transport proteins, which are involved in the transport of iron and other metals. ZIP14, ZIP8, TRPC1, TRPC3, TRPC6, TRPML1, and TRPML6 are effective transporters for the transport of iron into the cell (*Knutson, 2019; Yao & Garland, 2005*). Besides this, L-type and T-type calcium channels are also non-selectively effective for iron and other divalent metals uptake (*Lopin et al., 2012 & Kumfu et al., 2016*).

ROS can occur in reactions catalyzed by the presence of free metals (*Nakamura et al.,2019*). The storage of free iron in ferritins prevents the formation of ROS through Fenton reactions inside the cell. Free irons that cannot be stored by ferritins in the cell begin to form ROS (*Merkofer et al., 2006*). Superoxide molecules, one of the intermediates of oxygen respiration, are converted into oxygen molecules and H_2O_2 by superoxide dismutase (*Li et al., 2020*). Then, hydrogen peroxide is converted into water and oxygen by catalase activity. However, in cases where catalase activity is low, and the amount of free iron is high, ferrous iron and H_2O_2 react to form ferric iron and hydroxyl radicals as called Fenton reaction following equation (*Li et al., 2020*).

$$Fe^{2+} + H_2O_2 \rightarrow Fe^{3+} + OH^{\cdot} + OH^{-}$$

Then, these hydroxyl radicals react again with H_2O_2, resulting in the formation of superoxide (*Dimitrios et al., 2019*). Then forming superoxide also gives a reaction with H_2O_2 to form hydroxyl radicals and hydroxyl anion (Haber -Weiss reaction). In ferric form irons formed because of the reaction, it reacts with superoxide and forms iron in the ferrous form again. The hydroxyl radicals formed then react with all kinds of biomolecules, including nucleic acids, lipids, amino acids, inside the cell, resulting in irreversible cell damage (*Merkofer et al., 2006*).

1.2. Deficiency of Ferrous Iron (Fe^{2+}) and Vitamin C in Cultured Cells

The amount of iron in the plasma ranges from 10 to 30 µM under physiological conditions (*Ganz & Nemeth, 2011*). However, cell culture media contains ferric and/or ferrous iron levels well below this concentration range (*Spasojevic, 2016*). Serum (FCS or FBS) added to media are not also sufficient to provide the same concentrations of iron and Vitamin C in cultured cells as in vivo conditions (*Kakuta et al., 1997*).

Vitamin C is a water-soluble antioxidant that works as a cofactor in enzymes involved in many metabolic activities such as redox homeostasis and gene expression (*Zhitkovich, 2021*). It is also an effective ROS scavenger in detoxifying reactive oxygen species formed in cells so, its deficiency has a significant effect on the functions in the cell (*Chen et al., 2021*). Vitamin C enters the cell via sodium-ascorbate co-transporters (SVCT1 and SVCT2) while dehydroascorbic acid which is the oxidized form of Vitamin C enters the cell with different glucose transporters (GLUT1, GLUT3, and GLUT4) (*Zhitkovich, 2021*). After entering the cell in the form of dehydroascorbic acid, it enters the mitochondria via GLUT1 and GLUT10 and is converted back to Vitamin C as a mitochondrial ROS scavenger (*Zhitkovich, 2021*). It also reduces iron in the ferric form to ferrous form and allows iron to be taken into the cell through DMT1 (*Timoshnikov et al., 2020*). Vitamin C can exist in some cell culture media as ascorbate-2 phosphate in low amounts (*Azquate et al., 2013*). It does not have redox activity and can be oxidized quickly (*Michel & Frei, 2013*). The absence of vitamin C in the media also leads to changes in cell processes and stress resistance compared to in vivo (*Fedeles et al., 2015*). Vitamin C provided with serums does not meet the physiological level of 50-100 µM.

While Vitamin C is 1-5 mM in vivo in physiological conditions, it may require 10 mM and above in different cell types such as neurons and stem cells (*Zhitkovich, 2021*). Since cells can take Vitamin C in both reduced and oxide form, it can be supplemented in both forms (*Lorincz et al., 2019*). However, prolonged high-concentration Vitamin C supplementation under cell culture conditions is toxic to cells thus the optimum concentration of Vitamin C to be supplemented should be determined according to the cell type (*Duarte & Lunec, 2005*).

Cell culture contains 5% CO_2 and 95% air and this is another problem because cultured cells cannot effectively take up reduced iron and vitamin C (*Spasojevic, 2016*). This is the hyperoxic condition for cultured cells compared to in vivo. This can lead to ROS generation and cytotoxicity (*Chen et al., 2005*).

Vitamin C is also known for its anti-cancer effects (*Parrow et al., 2013*). Cancer cell lines cultured with low-iron cell culture media under oxygen-rich incubator kill because of diffusion of accumulated H_2O_2 in the presence of excess Vitamin C (*Mojic et al., 2014*). However, iron supplementation to cell culture media reverses this anticancer effect of Vitamin C (*Chen et al., 2005*). The amount of oxygen, which decreases in parallel with the accumulated H_2O_2, enables the iron to transform into a ferrous form, resulting in the reaction of iron in ferrous form with H_2O_2 and it starts to produce hydroxy radicals with lower diffusion, and cells are not affected in this situation (*Khan & Martell, 1967*).

1.3. Intracellular Iron Detection Methods

1.3.1. Ferrozine

Ferrozine assay is a simple, and rapid colorimetric technique used for iron determination. Ferrozine, which is also known as 3-(Pyridin-2-yl)-5,6-bis(4-sulfophenyl)-1,2,4-triazine disodium salt, is a water-soluble chromogenic chelator that contains pyridyl and phenyl sulfonate groups (*Stookey, 1970*). Ferrozine can only detect ferrous iron, not ferric iron therefore, in the principle of the assay, reducing agents such as ascorbic acid are used to reduce the iron in the sample (*Ring et al., 2018*).

The reaction of the chelating motif in the structure of ferrozine with ferrous iron forms a colored complex (*Hirayama & Nagasawa, 2017*). The color intensity of the complex formed is directly proportional to the amount of ferrous iron in the sample (*Vershoor & Molot, 2013*) and this color change provides to measure iron quantitatively at 562 nm.

Once iron enters the cell, it is stored by ferritin or forms a complex with related proteins (*Riemer et al., 2004*). Ferrozine is also used to measure the amount of ferrous iron in biological samples as in solutions. However, at this stage, the release of iron from these proteins should be performed using compounds such as acidic $KMnO_4$ before ferrozine assay (*Fish, 1988*). Then, the concentration of iron in the biological sample can be obtained by reacting the released ferrous iron with ferrozine (*Riemer et al., 2014*).

1.3.2. Perls/DAB Staining

Perls Prussian Blue staining is a quick, simple, and inexpensive technique for the investigation of iron distribution in tissue or subcellular levels of cells (*Roschzttadtz et al., 2010*). In this technique, a specific dye is not be used instead, the blue pigment is formed in the tissue or cell in the presence of ferric or ferrous iron pigments (*Meguro et al., 2007*). Potassium ferrocyanide, which is known as soluble Perls reagent, reacts with ferric iron, resulting in the forming of insoluble Prussian Blue pigment in dilute hydrochloric acid solution which liberates bound ferric iron from proteins and, these deposits can be visualized using microscopy (*Roschzttardtz et al., 2010*).

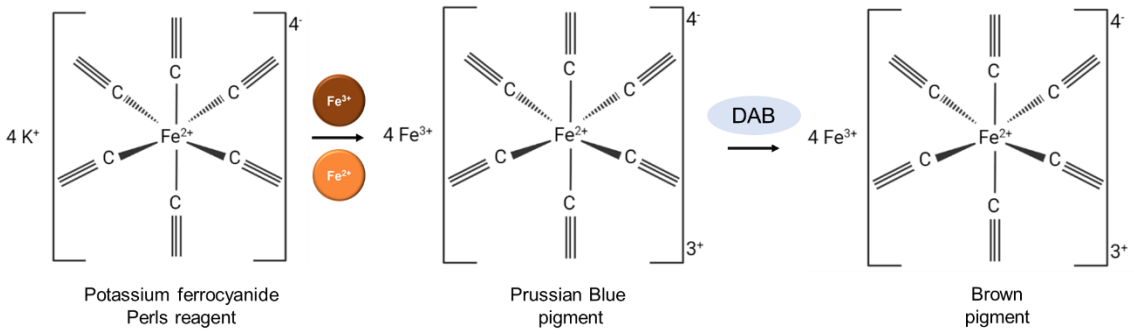

Figure 1. 2. Working principle of Perls/DAB staining for iron detection

Perls/DAB staining is also used for the distribution of iron in both tissue and cells

(*Meguro et al., 2007*). In this time, diaminobenzidine (DAB) and hydrogen peroxide (H_2O_2) are used to increase the staining sensitivity because of the low penetration between tissues and low sensitivity (*Nguyen-Legros et al., 1980*). After reacting potassium ferrocyanide with ferric iron, a redox-active complex form and this complex trigger the oxidative polymerization of DAB by H_2O_2, resulting in brown (*Nguyen-Legros et al., 1980*).

1.3.3. Inductively Coupled Plasma Mass Spectrometry (ICP-MS)

ICP-MS is a common analytical technique that can simultaneously measure many elements in low concentrations and contains an inductively coupled plasma source and mass spectrometer, which are used to ionize the sample to be analyzed (*Wilschefski & Baxter, 2019*). The samples to be analyzed in ICP-MS are converted into solution using appropriate solvent and then digested with the help of high purity acids (HNO_3, HCl, HF, etc.). The prepared solution is transferred to the ionization unit (plasma) with a carrier gas (usually argon). The sample is ionized there at a high temperature (10000 Kelvin). Ionizing elements are then determined in a mass spectrometer based on their mass/charge ratio. The resulting mass/charge ratio is digitized by the detector. ICP-MS is a widely used technique for heavy metal poisoning in the medical field. It can also be used to detect different isotopes of elements in water and soils.

Elemental analysis is performed in single cells using an ICP-based technique for element determination in biological samples and in this technique, called single-cell ICP-MS, a quantitative analysis of elements in a single cell is performed (*Meyer et al., 2018*). ICP-MS which requires expertise, is an expensive method, since argon gas is used, which is another disadvantage that restricts its use (*Meyer et al., 2018*).

1.3.4. Transmission Electron Microscopy (TEM)

Electron microscopes are microscopes in which imaging is provided by electron beams emitted, they allow the examination of many structures and microorganisms at a magnification of one million times (*Franken et al., 2020*). In addition, since the electron wavelength is shorter than the light wavelength, it has a higher separation power compared to the light microscope. Transmission electron microscope (TEM) uses a high

voltage electron beam and images are obtained by electron permeability of the samples (*Malatesta, 2021*). It is used for element determination in biological samples, including the distribution of localized iron at the subcellular level. It also gives information about the analysis of the difference in iron distribution between pathological and physiological tissues (*Franken et al., 2020*).

As a general procedure, the sample is usually embedded in a resin block, and then very thin sections are taken with the aid of an ultramicrotome, typically less than 200 nm (*Franken et al., 2020*). In addition, TEM samples of biological tissues require staining to increase contrast. Perls/DAB and Turnbull staining are some staining methods that provide high-resolution microscopic images to get information about the oxidation and distribution of iron in the cell.

1.3.5. Fluorescent Probes for Live-Cell Imaging of Fe^{2+}/Fe^{3+}

1.3.5.1. FeRhoNox-1

FerhoNox-1 is one of the limited numbers of turn-on fluorescent probes used to detect intracellular ferrous iron (Fe^{2+}) in imaging studies (*Hirayama et al., 2013*). The working principle of this probe depends on the de-oxygenation reaction of N-oxide modified rhodamine B in the presence of ferrous iron, resulting in fluorescence increasing irreversibly (*Hirayama et al., 2013*).

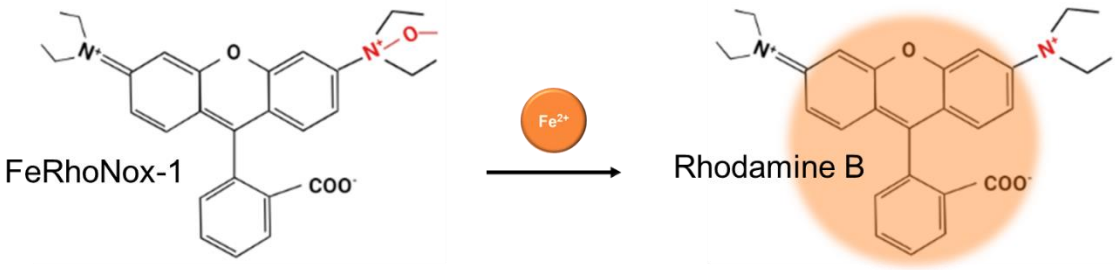

Figure 1. 3. Working principle of FeRhoNox-1

This probe, which response to Fe^{2+} with high selectivity, is ideal for the determination of both exogenous and endogenous ferrous iron in living cells using fluorescence microscopy or fluorometer at around 570 nm (*Hirayama & Nagasawa, 2017*). As a

disadvantage, this probe is localized to the Golgi apparatus or a small region of the endoplasmic reticulum. In addition, many versions have been developed and Fe^{2+} determination has been made possible at subcellular locales within the cell, for example, the accumulation of labile ferrous iron transported by transferrin to lysosomes with probes called HMRhoNox-M using hydroxymethyl rhodamine was visualized (*Niwa et al., 2014*).

1.3.5.2. Calcein-AM

Calcein-AM is used for detecting cellular labile iron (*Breuer et al., 1995*). It was formed by modifying acetomethoxy (AM) groups to the carboxylic acid groups of calcein (*Breuer et al., 1995*). This gain Calcein-AM hydrophobic properties to increase its penetration across the cell membrane and cytosolic esterases degrade this lipophilic compound after entering the cell (*Hirayama & Nagasawa, 2017*). In the case of the iron-binding, the green fluorescence signal of calcein decreases.

As with FeRhoNox-1, it is possible to monitor the flow of iron ions in the cell by using these probes (*Hirayama & Nagasawa, 2017*). Barely, this turn-off fluorescent probe has some disadvantages since ferrous iron bound to calcein is rapidly oxidized, this probe cannot distinguish between ferrous and ferric iron (*Tenopoulou et al., 2007*). At physiological pH, a decrease in the fluorescence signal is observed with the binding of other divalent metals such as manganese, nickel, copper, as it happens in iron. Besides, the binding of iron to calcein is pH dependent. Calcein-AM enters the cell and is rapidly converted to calcein. For this reason, calcein is kept inside the cell and it is not possible to enter the membrane-bounded cellular compartments like the lysosome, mitochondria, and endoplasmic reticulum (*Tenopoulou et al., 2007*). This property allows the measurement of labile iron only in the cytosol. However, it is not suitable for membrane-enclosed subcellular compartments. Also, iron binding to calcein is pH dependent for instance, lysosomes are known as organelles in which the amount of iron is high in the cell. The first reason is that calcein cannot pass through the lysosome membrane, and the second is about the low pH of the lysosome, resulting in not binding of calcein to iron.

1.4. Genetically Encoded Nitric Oxide Probes (geNOps)

Fluorescent proteins (FPs) have been applied in many scientific fields, especially in cell biology (*Kim et al., 2021*). FPs are designed with the help of protein engineering for genetically encoded biosensors (GEBs) designed to examine the interactions of molecules such as ions, metabolites, which have an important role in metabolic activities in living cells (*Chudakov et al., 2010*). Genetically encoded biosensors are powerful research tools that contain one or more FPs and an analyte, which is a specific domain of interest for detection (*Greenwald et al., 2018*). The spectral properties of the fluorescent protein change in response to the dynamic change that occurs because of the interaction of the analyte in the structure of these biosensors with the target molecule and are visualized with high-resolution live imaging techniques (*Depaoli et al., 2019*). Genetically encoded biosensors can be targeted to cell compartments such as mitochondria, nucleus, and plasma membrane using appropriate localization sequences within the cell (*Ren et al., 2013*). Genetically encoded biosensors that have a different degree of specificity and sensitivity (*Ren et al., 2013*) show off long-term stability under the microscope, resulting in increasing their use (*Arai et al., 2019*). Single FP-based biosensors, which are one of the commonly used genetically encoded biosensors, show fluorescence changes in their structure depending on the concentration of the target molecule bound to the analyte in the sensor (*Depaoli et al., 2019*).

Various genetically encoded biosensors have been developed that provide a direct or indirect measurement of nitric oxide, whose low concentration and high reactivity with other molecules make its measurement difficult, at the single-cell level (*Eroglu et al., 2018*). Genetically encoded NO probes, (geNOps), are constructed by fusing the C terminal of the GAF domain, which is a bacterium-derived NO binding domain of the transcription factor norR, with single fluorescent protein variants provide selectively real-time detection of nitric oxide dynamics in a single cell level (*Eroglu et al., 2016*). The conformational change of fluorescent protein resulting from the binding of nitric oxide to the GAF domain affects the electron density of chromophore, resulting in fluorescent-quenching (*Eroglu et al., 2016; Eroglu et al., 2018*). Genes that convert nitric oxide (NO) to nitrous oxide (N_2O) in E. coli and denitrification bacteria are controlled by the NorR transcription factor (*Spiro, 2007*). The enhancer-binding protein NorR has the N-terminal

GAF domain, the detection region for nitric oxide (*D'Autréaux et al., 2005*). Nitric oxide binds to the non-heme ferrous iron center in this domain (*Bush et al., 2015*). Nitric oxide binding to this center coordinated by side chains of three aspartate, one arginine, and one cysteine results in the formation of the mono-nitrosyl complex as a result of stimulation of ATPase activity (*Bush et al., 2011*).

geNOps are available in multicolor variants, cyan-green, and orange which are highly selective and sensitive to NO (*Eroglu et al., 2016*). geNOps are reversible and have fast on/off kinetics allowing the rapid visualization of low concentrations of nitric oxide (*Eroglu et al., 2016*). The responses of geNOps to endogenously produced NO and exogenously different NO donors in different cell types enable both to examine the functions of nitric oxide in the cell. In addition, geNOps are suitable for the measurement of nitric oxides produced from different nitric oxide isoforms (*Eroglu et al., 2017; Charoensin et al., 2017*). Since geNOps are small in size, they can be localized at different compartments in the same cell, and thus the simultaneous NO dynamics can be visualized (*Eroglu et al., 2016*). In addition, multicolor geNOps can be used with biosensors or chemical probes with different spectral properties. This simultaneously contributes to the investigation of related molecules such as calcium (*Opelt et al., 2017; Charoensin et al., 2017*). Due to many FPs being prone to pH fluctuations, fluorescent quenching occurs in the acidification of geNOps in the cyan and green variant while alkalization is also in the opposite direction of this case, resulting in fluorescent intensity increases (*Eroglu et al., 2016; Eroglu et al., 2018*).

2. AIM OF THE STUDY

Genetically encoded NO probes (geNOps) are metalloproteins consisting of a non-heme iron (II) center that is required for NO sensing. Acute iron (II) supplementation is an essential procedure for the full and accurate functionality of the probe in cultured cells. Thus, I hypothesized that such a metalloprotein might serve as a potential model system to test indirectly the iron (II) uptake in cultured cells for other iron-dependent metalloproteins. Within this scope, I aimed in this study to investigate:

1. whether geNOps are suitable as an indirect Fe^{2+} reporter,

2. the development of a culture media supplemented with different concentrations of Fe^{2+} and/or Vitamin C

3. imaging of the intracellular Fe^{2+}/Fe^{3+} distribution in cultured cells

4. optimization the Fe^{2+} provision procedure in cultured cells expressing geNOps.

3. MATERIALS

3.1. Chemicals

Chemicals used during this thesis study are categorized in **Appendix A.**

3.2. Equipment

All equipment used during this thesis study are categorized in **Appendix B.**

3.3. Molecular Biology Kits & Enzymes

Molecular Biology Kits and enzymes used during this thesis study are categorized in **Appendix C.**

4. METHODS

4.1. Bacterial Cell Culture

4.1.1. Transformation of Plasmids to Competent Bacteria

DH5α Competent *E. coli*, which is a common strain for routine cloning applications, were thawed on ice. 50 µl of bacteria were placed in a sterile microcentrifuge tube and chilled immediately. 3 µl of the desired plasmid DNA was added inside of the same tube and mixed them gently by pipetting up and down. The tube was placed on ice for 30 minutes without mixing. After 30 minutes, heat shock was applied to the same tube at 42 °C for 45 seconds and then the tube was incubated on ice for 10 minutes. 500 µl of LB media was added to the tube, and it was placed in the shaking incubator at 37 °C at 220 rpm for 60 minutes. During this time, a selection LB agar plate was warmed to 37 °C. After 1 hour, the mixture was spread on the LB agar plate and the plate was incubated at 37 °C overnight. A single colony was picked up and inoculated in 3 ml of LB agar with the appropriate antibiotic at 37 °C overnight. Then, the growing bacterial culture was mixed with 50% glycerol (v/v) as a ratio of 1:1. The prepared tubes were kept at -80 °C for long-term storage.

4.1.2. Midiprep Plasmid DNA Isolation

5 ml of LB media and 5 µl of an appropriate antibiotic were placed in a sterile 15 ml falcon. Pre-incubation was applied by adding 5 µl of glycerol stock of DNA of interest in a shaking incubator at 37 °C at 220 rpm for 3 hours. After this pre-incubation, the growing cell cultures were transferred into a sterile Erlenmeyer flask containing 50 ml of LB media and 50 µl of an appropriate antibiotic. Then, the flask was incubated in a shaking

incubator at 37 °C at 220 rpm overnight. After incubation, growing bacterial cell cultures were placed in a sterile falcon and centrifuged at 4 °C at 4700 rpm for 15 minutes. After obtaining the bacterial pellet, the plasmid DNA isolation process was applied using MidiPrep Kit (Qiagen, 12945) according to the manufacturer's instructions. The concentration and purity of obtained plasmid DNA were measured using nanodrop, and it was stored at 4 °C for further usage.

4.2. Mammalian Cell Culture

4.2.1. Cell Culture

Human embryonic kidney cells (HEK293T, ATCC® CRL-1573TM) were grown in a high-glucose (4.5 g/L) complete DMEM including 10% FBS (v/v) and 1% penicillin (100 U/ml) and streptomycin (100 µg/ml). Immortalized human umbilical vein endothelial cells (EA. hy926) were cultured in the same complete medium with additional supplements: 2% HAT supplement (consisting of 5 mM sodium hypoxanthine, 20 µM aminopterin, and 0.8 mM thymidine) and 100 µg/ml normocin.

Cells were seeded in 10 cm cultures dishes and incubated in a humidified incubator at 37 °C with 5% CO_2. The cells were passaged when they reach 80-90% confluency to enable their further proliferation. Cells were washed one time with Dulbecco's Phosphate Saline Buffer (DPBS) and 1 ml of trypsin-EDTA was added. Then, the plate was incubated in the incubator for an appropriate time (depending on the cell line) to detach the cells from the vessel. DMEM was added to inactivate the trypsin, and media with cells was collected in a 15 ml falcon. New cell cultures plates were prepared as 1:5 or 1:10 in new 10 cm plates.

4.2.2. Transient Transfection of HEK293T cells

For imaging experiments on a wide-field microscope, cells were seeded (~3-5 x 10^5 cells per well) on 30 mm glass coverslips placed in a 6-well plate. At ~80–90% confluency, cells were transfected using PolyJet transfection reagent according to the manufacturer's

instructions. All imaging experiments were performed 16-24 h after transfection.

The confluency of HEK293T cells seeded into a 6-well plate 1 day before was checked. When the cells reached approximately 80-90% confluency, the cell culture medium was changed with a fresh one. Two clean Eppendorf was taken and labeled as DNA and PolyJet. 50 µl/well serum and phenol red-free DMEM medium and 1 µg/well DNA of interest was added into the DNA labeled tube. Inside of the PolyJet labeled tube, 50 µl/well serum-free phenol-red free DMEM and 2 µl/well PolyJet which is an in vitro transfection reagent were added. After adding PolyJet inside of the tube, the mixture was slowly and gently mixed by pipetting up and down and the whole mixture was added into the DNA tube. This transfection mixture was incubated for 15 min at room temperature. Afterward, 100 µl of the mixture was added into one well of a 6-well plate. Cells were incubated with the transfection solution in a humidified chamber at 37 °C 5% CO_2 for 3 hours. After 3 hours, the medium containing the transfection mixture was replaced with a fresh medium. After 16-24 hours, cells were ready for live-cell imaging.

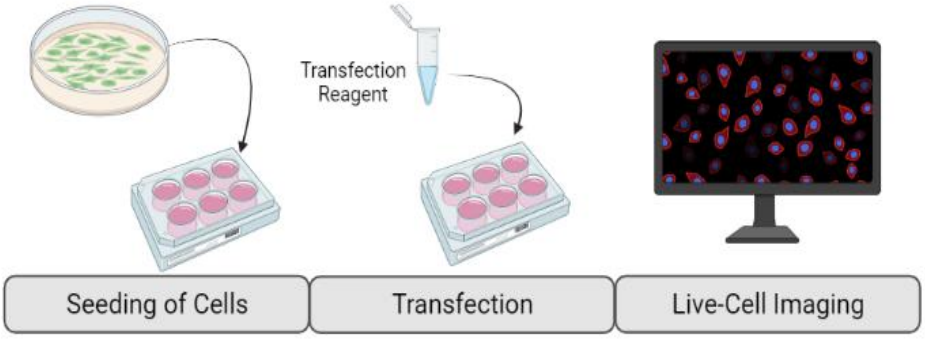

Figure 4.1. Process of transient transfection, which is used for a short period, no passing to future generations of the cell.

4.2.3. Stable Cell Line Generation

Cytosol targeted O-geNOp (O-geNOp-NES) construct was subcloned into a 3rd generation lentivirus shuttle vector pLenti-MP2 (Addgene #36097) by using the following primers: forward 5'-ATAGGATCCGCCACCATGGTGAGTGTG-3' including BamHI restriction site and reverse 5'-ATAGTCGACTTACAAAGTCAATCTTTCT-3' including a stop codon and SalI restriction site The plasmid was amplified in the chemically competent Stbl3 bacteria. HEK293T cells were used to generate lentivirus particles. At 80-90% confluency cells

were co-transfected with 3µg psPAX2, 3µg pMD2.G, and 6µg O-geNOp-NES lentivirus shuttle vector using PolyJet transfection reagent according to the manufacturer's instructions. After 24h, the transfection medium was replaced by fresh DMEM. After further 24h and 48h incubation, the cell culture medium containing virus particles was collected and filtered using a 0.45µm low protein binding medium filter and subsequently ultra-filtrated using a 100 kDa Amicon® Ultra-15 Centrifugal Filter Unit at 4 °C with 3000 x g for 30 min to concentrate the lentivirus particles. Filtrates were aliquoted and immediately used or snap-frozen in liquid nitrogen and stored at -80 °C. For stable cell line generation, EA. hy926 cells were seeded on 6-well plates and allowed to attach before replacing the antibiotic-free transduction medium containing 10% FBS, 10 µg/ml Polybrene infection reagent, and lentivirus particles encoding for cytosol targeted O-geNOps. Optimization of lentiviral transduction was achieved by using serial dilutions of the viral particle containing filtrates. Cells were maintained in the virus-containing medium for 48h-72h. After positive transduction, cells were further cultured for one week in fresh complete DMEM before fluorescence assisted cell sorting (FACS). Top 30% of O-geNOp-NES positive cells were selected by detecting the red fluorescence emission using an excitation wavelength of 561 nm laser (Filter type: BP 593/40 nm) on a B.D. Influx Cell Sorter. Sorted EA. hy926 cells consisting of positively transduced cells were regularly maintained under cell culture conditions before imaging experiments. Stable EA. hy926 cells expressing O-geNOp-NES were seeded on 30 mm glass coverslips one day before the imaging experiment.

4.3. Buffer Preparation and Colorimetric Fe^{2+} Detection

4.3.1. Preparation of Storage Buffer

Prior to imaging experiments, cells were incubated at room temperature in a cell storage buffer called an EH-loading (EHL) buffer. EHL buffer functions as a DMEM as it contains all components except FBS and phenol-red. For this reason, it helps cells adapt to the external environment during the imaging experiment. EHL buffer consists of 138 mM NaCl, 2 mM $CaCl_2$, 5 mM KCl, 1 mM $MgCl_2$, 1 mM HEPES, 2.6 mM $NaHCO_3$, 0.44 mM KH_2PO_4, 0.34 mM Na_2HPO_4, 10 mM D-glucose, 0.1% MEM vitamins, 0.2%

essential amino acids, and 1% penicillin/streptomycin. The desired volume was completed with distilled water. The pH of the solution was adjusted as 7.4 using 1 mM of NaOH. Then, the complete solution was filtered using a 0.22 µm filter to make it sterile. Solution filtered was aliquoted and stored at 4 °C for further usages. EA. hy926 cells stably expressing O-geNOp-NES were kept in EHL buffer maximum of 30 minutes, while HEK293T cells were for 2 hours.

4.3.2. Preparation of Imaging Buffer

In live-cell imaging experiments, HEPES-buffered physiological salt solution consisting of 138 mM NaCl, 5 mM KCl, 2 mM $CaCl_2$, 1 mM $MgCl_2$, 10 mM D-glucose, 10 mM HEPES was prepared. All imaging buffers were adjusted to pH 7.4 by using 1 M NaOH. In addition, all stimulators such as NOC-7 used during the experiment were prepared in this physiological buffer.

4.3.3. Preparation of Iron (II) Solution

For geNOps functionality, cultured cells were incubated in a physiological buffer containing iron (II) sulfate and Vitamin C. 1 mM of $FeSO_4$ and 1 mM Vitamin C was added into the physiological buffer and mixed with vortex for approximately 1 minute. Then, the solution was filtered by using a 0.22 µm filter and immediately used for the treatment of cells. Cells were treated with this iron (II) solution and incubated in a humidified chamber at 37 °C with 5% CO_2 for 20 minutes. After incubation, cells were washed with PBS, and EHL storage buffer was added for real-time live cell NO imaging experiments. When only iron (II) fumarate was used as an iron source, Vitamin C, and iron (II) fumarate added to the buffer were mixed on a magnetic stirrer for 2 hours. It was then filtered. For $FeSO_4$ and $FeCl_2$, protocol steps were applied respectively without using a magnetic stirrer (**Figure 4.2.**).

All iron solution treatments made in this thesis study were prepared by following this protocol, only the concentrations used, and incubation times were changed. Stability test done by $FeSO_4$ showed that $FeSO_4$ can also be used after 1 day but as a small suggestion it will be better to prepare it fresh before the imaging experiment.

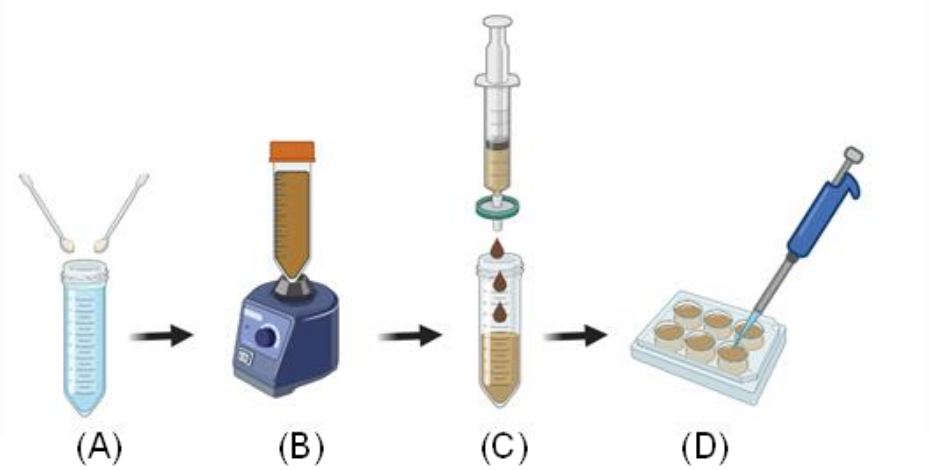

Figure 4.2. Preparation of iron (II) solution for the incubation of cells before the imaging experiment. (A) Adding of appropriate concentration of FeSO4 and Vitamin C (B) Mixing the solution via vortex (C) Filtering of the solution for sterilization (D) Treatment of the cells with the prepared solution.

4.3.4. Ferrozine Assay

Ferrozine assay was applied to detect iron (II) in solution quantitatively. Standard solutions and samples were prepared. Then, all samples were diluted as 1:50. 60 µl of iron detection reagent was added into these diluted samples and 15 minutes of incubation was applied at room temperature protecting light. After incubation time, absorbance values were collected at 562 nm using a UV-visible spectrophotometer, and a standard curve was drawn according to the values of the standard solutions. According to the reference curve, the iron concentration of samples was determined.

4.4. Staining

4.4.1. Perls/DAB Staining

Perls/DAB staining of iron particles was applied by using the previously published protocols described elsewhere was applied (*Meguro et al., 2007; Sheehan et al., 1980*). The cells were treated with iron (II) solution according to the appropriate concentration of $FeSO_4$ and/or Vitamin C and incubation times. After treatment, cells were washed with distilled water and fixed with Karnovsky fixative solution for 30 minutes. After fixation,

cells were treated with the mixture of the same volume of 2% HCl and 2% potassium ferrocyanide ($K_3Fe(CN)_6$) for 30 minutes. After washing with distilled water, 0.01 M sodium azide (NaN_3) in 0.3% H_2O_2 solution was added onto the cells for 30 minutes. This step was followed by DAB intensification, which includes 30 minutes of incubation in a solution consisting of 0.025% DAB and 0.005% H_2O_2. As the last step, cells were washed with distilled water to stop the reaction. After treatment with iron (II) solution, all following steps were performed at room temperature. Cells were imaged on a confocal light microscope LSM800 to detect iron particles in cells stained with Perls/DAB solution.

4.4.2. FeRhoNox-1 and Hoechst Co-Staining

Cultured cells with 70-80% confluency was incubated with physiological buffer (pH 7.4) containing indicated concentrations of iron (II) sulfate ($FeSO_4$) and/or Vitamin C and incubation time in a CO_2 regulated incubator before imaging. After incubation, cells were washed with warm PBS, and Hoechst and FeRhoNox™-1 co-imaging was performed. Cells were stained with 5 µg/ml FeRhoNox™-1 in the physiological buffer for 60 minutes at 37 °C and 5% CO_2. Subsequently, cells were washed with warm PBS, and further incubated for 15 min with 10 µg/ml Hoechst at 37 °C and 5% CO_2. Prior to imaging, cells were again washed with warm PBS and incubated in storage EHL buffer. Cells were imaged by using high-resolution laser scanning confocal light microscope LSM800.

4.4.3. Cell Apoptotic Assay: Hoechst and Propidium Iodide (PI) Staining

Propidium iodide (PI) and Hoechst co-staining were applied to mark dead cells and nuclei, respectively. Firstly, cells were treated with the physiological buffer containing the desired concentration of $FeSO_4$ and/or Vitamin C in indicated incubation times at 37 °C 5% CO_2. After incubation, cells were washed one time with PBS. Then, cells were stained with 10 µg/ml Hoechst prepared in physiological buffer and incubated at 37 °C 5% CO_2 for 15 minutes. Afterward, cells were washed with warm PBS. Cells were co-stained with 5 µg/ml PI prepared in physiological buffer and incubated at 37 °C 5% CO_2 for 10 minutes. Cell imaging was performed on a wide-field epifluorescence microscope equipped with a Plan-Apochromat 20x/0.8 M27 objective. Cells stained with PI were excited using a 561 nm laser, and respective emission light between 595-700 nm was

collected using GaAsP-PMT. Hoechst labeled cells were excited using 405 nm laser light, and emission was collected using Multialkali-PMT between 410-546 nm.

4.5. Live-Cell Imaging

4.5.1. Real-Time Fluorescence Imaging

Real-time cell imaging experiments were performed on inverted wide-field epifluorescent microscopes, either an Axio Observer.Z1/7 or Axio Vert.A1 (Zeiss, Germany). These microscopes are equipped with a Plan-Apochromat 20x/0.8 dry objective, a Plan-Apochromat 40x/1.4 DIC (UV) VIR-IR oil immersion objective, and monochrome CCD cameras Axiocam 503. Axio Observer.Z1/7 was equipped with an LED light source Colibri 7 R[C/Y] CBV-UV and Axio Vert.A1 with an LED light source Colibri 2 (365nm, 470 nm, 625nm). O-geNOps expressing cells were excited with the excitation wavelength of 555/30 nm using LED modules of Colibri 7 and emission was collected using the filter combinations FT570 (B.S.) and emission filter 605/70: Intensiometric O-geNOps imaging on Axio Vert.A1 was excited with the Colibri 2 LED module 555 nm and emission were collected with the filter cube combination number 43 (DsRed). Data acquisition and control on both imaging systems was carried out using the Zen Blue 3.1 software (Zeiss, Germany). Camera binning for real-time imaging was set to 4x4, light intensities were adjusted between 3%- 10% for HEK293 cells and 70%-100% for stably O-geNOps expressing EA. hy926 cells, exposure times were adjusted according to the expression rate set between 30 ms and 300 ms. A Neutral-Density filter (N=0.06) was used in all imaging experiments.

4.5.2. Gravity-based Perfusion System

All imaging experiments were performed using a gravity-based or pump-driven custom perfusion system to supply or withdraw drugs or substrates to the cells. The perfusion system includes the syringe tubes in which the solutions required for the stimulation of the cells are put, the manual or automatic on-off switches used to ensure the flow of the fluid in the tubes, and the plastic capillary tubes through which the fluid flows. The metal

perfusion chamber where the cell is placed has two sides, one inlet and one outlet. The inlet part is connected to the capillary tube, which is connected to the syringe with the stimulators, while the outlet part is connected to the vacuum pump. While the cells are stimulated with the inlet part, the liquid accumulated in the chamber is drawn with the vacuum pump and transferred to an empty container.

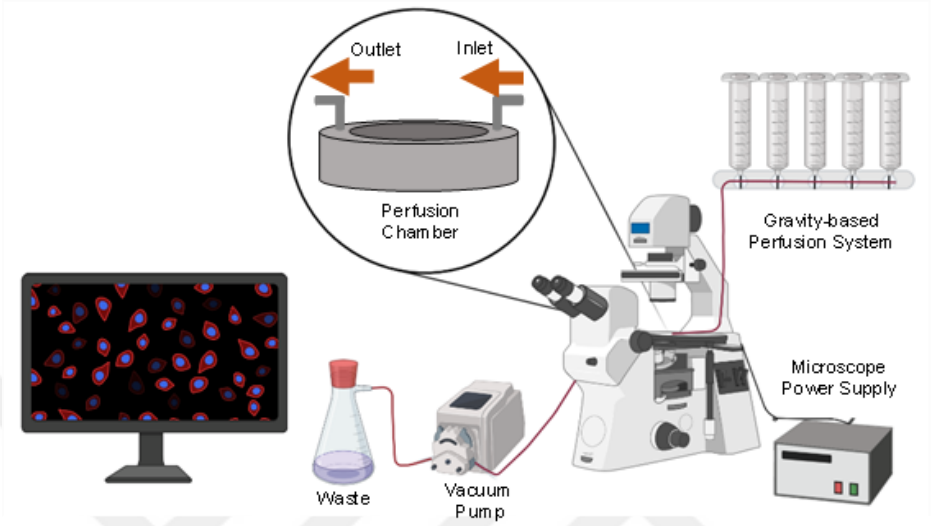

Figure 4.3. Gravity-based perfusion system for live-cell imaging experiment. This figure is a simple illustration of the gravity-based perfusion system used in live-cell imaging experiments. The most important part is the gravity-based reservoirs with the stimulators that change according to the experiment and that it contains during the experiment. During the experiment, the reactions of the cells by the chemicals present here are observed in real-time with the help of fluorescence microscope. The perfusion chamber, which allows the liquids in the reservoirs to be transferred to the cell, contains two inlets, an outlet, and an inlet. While the inlet part of this chamber, which has a 30 mm cover glass containing cells, is connected to the reservoir, the outlet part provides the output of the liquids given with the help of the vacuum pump, and these liquids are collected in a flask during the experiment in the waste.

4.5.3. High-Resolution Confocal Microscopy

High-resolution, bright-field confocal images were taken using a laser scanning confocal microscope LSM 800 (Zeiss, Germany) equipped with a Plan-Apochromat 40x/1.3 DIC (UV) VIS-IS oil immersion objective. 1024x1024 image size pixels were used, and averaging was set at 4 to achieve high-resolution images. FeRhoNox™-1 labeled cells were excited using 561 nm with 8.00% laser intensity and 850 V detector gain. Respective emission light between 555 nm and 700 nm was collected using GaAsP-PMT. The Hoechst dye was excited using 405 nm with a 3.50% laser intensity and 650 V detector gain. Respective emission light between 400 and 555 nm was detected using Multialkali-

PMT. Phase-contrast images for each sample were also taken using a Photodiode detector. The digital detector gains and pinhole size for all channels were set to 1 and 35 µm, respectively.

Z-stacks for each sample from the upper limit to the bottom of the cell were taken, and approximately ten slices (1 µm thickness) were imaged. The intensity of cells stained with FeRhoNox-1 and the cell numbers were collected with the help of the software. The intensity values obtained were divided into cell numbers, and normalizing graphed all conditions. Regions of interest were selected and processed using Zen Blue 3.1 software (Zeiss, Germany).

4.6. Statistical Analysis

All acquired imaging data were analysed using GraphPad Prism software version 5.04 (GraphPad Software, San Diego, CA, U.S.A.). All experiments were repeated at least three times in different cell cultures. The number of experiments was given as 'N', and the total number of cells imaged was indicated as 'n.' For instance, n=3/18 indicates that the experiment was repeated 3 times, and a total of 18 cells was selected and analysed. All statistical data were presented as mean ±SD and the representative real-time traces were shown as curves (if not indicated otherwise). Statistical comparison of two groups was evaluated using a two-tailed student t-test. Statistical comparisons of multiple groups, one-way ANOVA analyses of variances with post-test Dunnett's Multiple Comparison Test (comparison of all pairs of columns to control) were performed.

5. RESULTS

5.1. geNOps are suitable as an indirect iron (II) reporter

We hypothesized that these probes might be a suitable model system to visualize ferrous iron content in cultured cells because geNOps are metalloproteins. For this purpose, we used a mammalian codon-usage optimized variant of the orange version of geNOps, termed O-geNOps as the model system for a metalloprotein. We utilized HEK293T cells as a model cell organism. As shown in **Figure 5.1A,** transient transfection of HEK293T cells yielded high transfection and expression efficiency. Administration of NOC-7, a potent NO donor to cells, only showed a weak geNOps response without any treatment (**Figure 5.1B**). However, cell pretreatment with 1 mM of iron (II) fumarate and 1 mM of vitamin C resulted in a robust and instant geNOp signal responding to the NO-donor, NOC-7 (**Figure 5.1.B**).

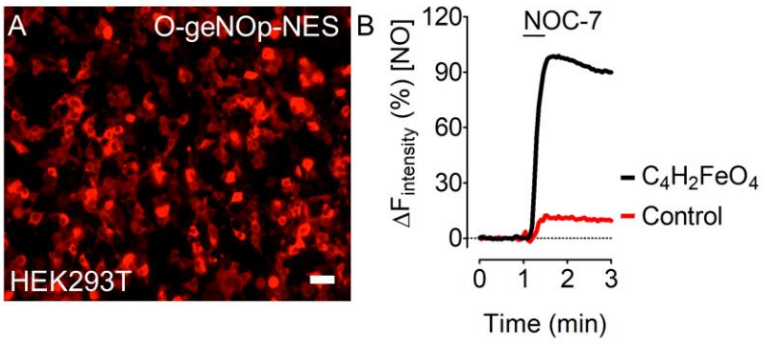

Figure 5.1. The functionality of geNOps to NOC-7 requires iron (II) fumarate treatment. (A) The panel shows the representative wide-field image of HEK293T cells expressing O-geNOp NES. The image was obtained from one channel (555 nm/610 nm). Scale bar represents 20 μm. **(B)** The black curve in the panel demonstrates the average NO response of HEK293T cells expressing O-geNOp-NES to 10 μM NOC-7 upon treatment with 1 mM iron (II) fumarate ($C_4H_2FeO_4$) and 1 mM Vitamin C (n=3/123). Cells were treated with this indicated iron solution for 20 min. The red curve in the same panel points out the NO response without treatment indicated as a control (n=3/70).

This data demonstrates that geNOps require reduced iron (II) supplementation for proper functionality and suggests that these probes can be indirectly utilized to test the functionality of metalloprotein in the presence or absence of intracellular iron.

Iron (II) fumarate provision to cells expressing geNOps has turned to a gold standard. However, iron (II) fumarate is a hardly soluble compound that requires vigorous mechanical stirring in a physiological salt solution over two hours. In **Figure 2**, we examined the solubility of iron (II) fumarate in a physiological buffer solution. We utilized the well-established ferrozine method to determine the dissolved iron (II) content in the physiological salt solution (**Figure 5.2A**). As shown in **Figure 5.2B,** at least 2 hours of vigorous mechanical mixing is required to dissolve iron (II) fumarate in the physiological buffer.

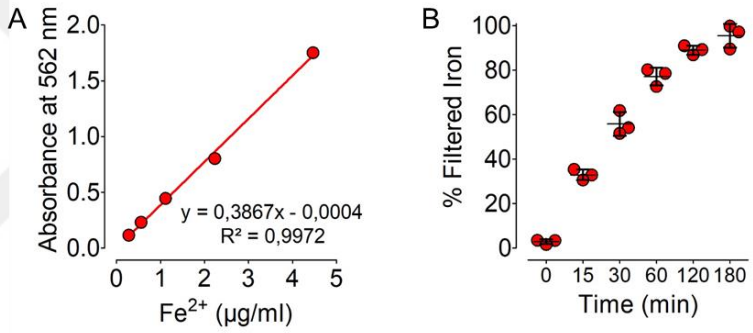

Figure 5.2. The solubility of iron (II) fumarate necessitates mechanical stirring. (A) Fe^{2+}-ferrozine complex standard curve procured with increasing concentrations of $FeSO_4$ (0, 100, 200, 400, and 800 µM $FeSO_4$). Each concentration has been recorded in triplicates. The correlation coefficient was 0.997 obtained from concentration ranges. **(B)** Time course represents the solubility of iron (II) fumarate upon stirring after 15, 30, 60, 120, and 180 minutes, respectively. Soluble iron (II) was determined using a Ferrozine assay. All experiments were repeated three times as are represented as ±SD.

To distangle the iron (II) provision from this limitation, we investigated whether other ferrous iron compounds may activate geNOps functionality. For this purpose, we compared $FeSO_4$ and $FeCl_2$ against iron (II) fumarate and again measured NO responses in HEK293T cells expressing O-geNOp-NES. Unlike iron (II) fumarate, $FeSO_4$ and $FeCl_2$ readily dissolved in the physiological buffer solution allowing direct use of it without mechanical stirring. As shown in **Figure 5.3A**, cell treatment with all three ferrous iron compounds containing the 1 mM of Vitamin C yielded comparable geNOps signals in response to NOC-7. While all ferrous iron compounds showed a significant difference

compared to control, a significant difference was not observed between the maximum responses of $FeSO_4$ and $FeCl_2$ used compared to iron (II) fumarate (**Figure 5.3B**). These data clearly show that also other ferrous iron compounds can readily enter cells to activate geNOps as well as iron (II) fumarate.

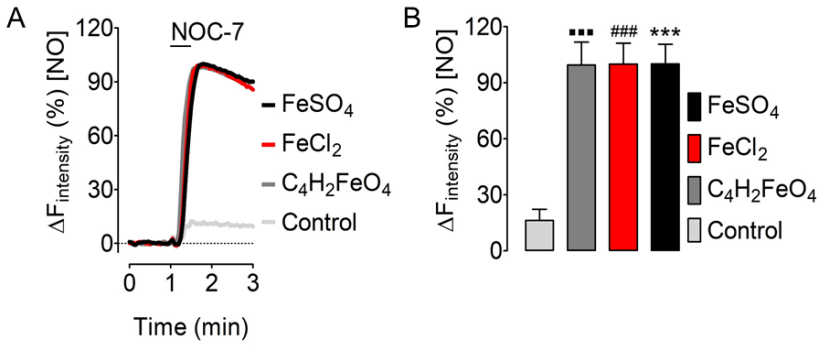

Figure 5.3. Different iron (II) compounds yield similar NO responses in geNOps. (A) Representative real-time traces of HEK293T cells in response to 10 µM NOC-7 upon either treated with $C_4H_2FeO_4$ (dark grey curve), $FeCl_2$ (red curve), $FeSO_4$ (black curve), or control with no treatment (light grey curve). All iron solutions contain 1 mM Vitamin C as a reducing agent. **(B)** The bars represent the maximum NO responses of O-geNOp-NES pre-treated with 1 mM $C_4H_2FeO_4$ (dark grey bar, n=3/123), $FeCl_2$ (red bar, n=3/150), $FeSO_4$ (black bar, n=3/189), respectively, or control without any treatment (light grey bar, n=3/70). Dunnett's Multiple Comparison Test was applied to compare all columns to the control column. All values denote mean ±SD of measurements in at least 3 different cell cultures. P-value summary: *$p<0.0001$* (Control vs $C_4H_2FeO_4$ ▪▪▪, Control vs $FeCl_2$ ###, Control vs $FeSO_4$ ***).

We next tested the stability of iron (II) fumarate, $FeSO_4$, and $FeCl_2$ on geNOps functionality by comparing the NO signals upon cell treatment with freshly prepared iron (II) buffers vs. 24 hours or 1-week old solutions. Our results attest that iron (II) fumarate treated cells displayed significantly reduced NO signals when treated with iron (II) fumarate solution that has been prepared 24 hours before cell treatment (**Figure 5.4A**), indicating the oxidation of iron (II) fumarate. The same result was observed in iron (II) fumarate, which was prepared 1 week before (**Figure 5.4D**). The statistical analysis of maximum NO responses in both conditions for iron (II) fumarate showed a significant difference (**Figure 5.4A, D**). In contrast, $FeCl_2$ treated cells yielded stable NO signals when treated with 24 hours old iron (II) solutions, yet cell treatment with an iron (II) solution stored for one week significantly reduced geNOps performance (**Figure 5.4B, E**). Compared to other ferrous iron compounds, $FeSO_4$ treated cells showed the most dramatic NO responses even when treated with a 1-day-old or 1-week-old iron (II)

solution (**Figure 5.4C, F)**. Consequently, we continued to apply $FeSO_4$ in further investigations due to the stability of $FeSO_4$ in solution compared to the other compounds.

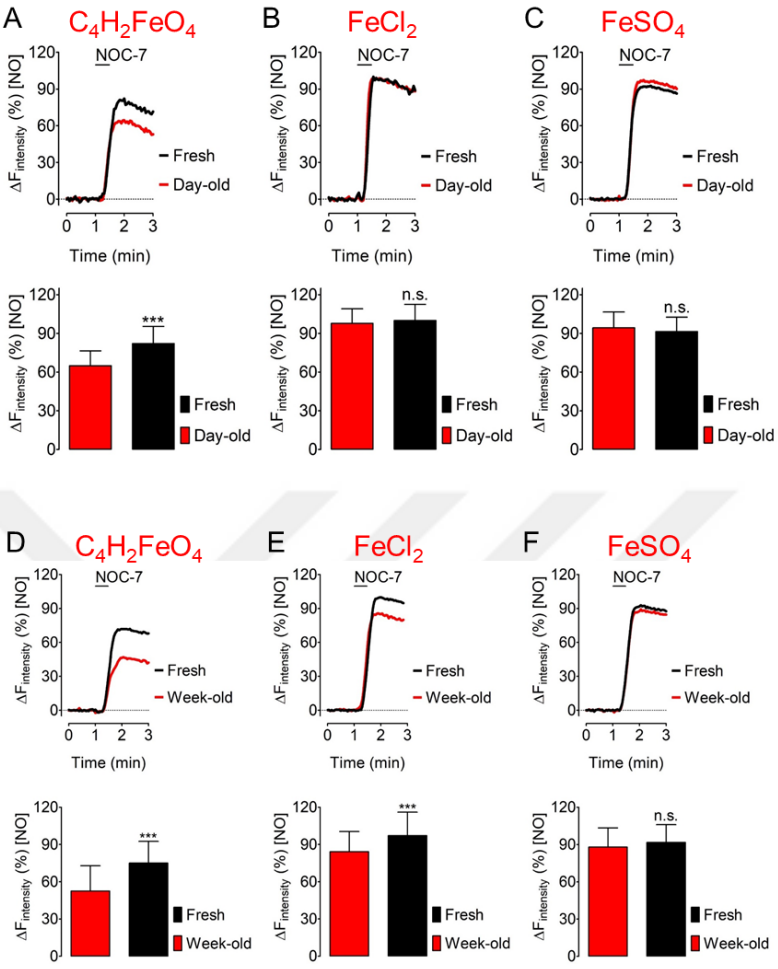

Figure 5.4. $FeSO_4$ is more stable than other ferrous iron compounds. (A) The upper panel shows real-time traces of intracellular NO signals in HEK293T cells expressing O-geNOp-NES in response to 10 µM NOC-7. The red curve indicates the response of cells treated with buffer containing iron (II) fumarate prepared one day ago while the black curve shows the same iron solution prepared freshly. Bars in the lower panel indicate the maximum response and statistical analysis of cells treated either one-day-old (red bar, n=3/93) or fresh (black bar, n=3/99) iron (II) fumarate. **(B)** The panel shows the same experimental setup as presented in panel A, except the iron source was $FeCl_2$. Red curves show NO signals of cells treated with buffer containing either one-day-old while black curve presents cell signals upon fresh $FeCl_2$ treatment. Bars show the maximum response of cells upon one-day-old (red bar, n=3/111) or fresh (black bar, n=3/106) $FeCl_2$ treatment. In panel **(C)** $FeSO_4$ was used as an iron source using the same experimental setup. The average NO responses were shown after administration of physiological buffer containing $FeSO_4$ prepared one day ago (red curve) or fresh (black curve). Bars display maximum response and statistical analysis against one-day-old (red bar, n=3/101) or fresh (black bar, n=3/100) $FeSO_4$ treatment. **(D)** Curves and bars show the average NO response and statistical analysis of maximum responses, respectively, upon treatment physiological buffer containing either one-week-old $C_4H_2FeO_4$ (red curve or bar, n=3/93) or fresh $C_4H_2FeO_4$ (black curve or bar, n=3/99). **(E)** Curves and bars show the average NO response and statistical analysis of maximum responses, respectively, upon treatment

physiological buffer containing either one-week-old $FeCl_2$ (red curve or bar, n=3/137) or fresh $FeCl_2$ (black curve or bar, n=3/110). **(F)** Curves and bars show the average NO response and statistical analysis of maximum responses, respectively, upon treatment physiological buffer containing either one-week-old $FeSO_4$ (red curve or bar, n=3/107) or fresh $FeSO_4$ (black curve or bar, n=3/101). All iron solutions contain 1 mM Vitamin C and old iron solutions were stored at 4 °C until experiment day. An unpaired t-test was applied for statistical analysis. All values denote mean ±SD of measurements in at least 3 different cell cultures. P-value summary: *p<0.0001*, ***.

Notably, cellular iron (II) uptake requires a reduced form of iron. In previous studies, the strong reducing agent vitamin C has been successfully applied. Therefore, we next tested different reducing agents including D-cysteine and GSH in comparison to Vitamin C. We observed that cells treated with Vitamin C yielded supplemented iron (II) solution yielded the most robust NO response in cells expressing geNOps (**Figure 5.5A**). All the reducing agents used showed a significant difference in the NO response compared to non-treated cells (**Figure 5.5B**). As a result, this study demonstrates that geNOps require a reducing agent for full functionality and demonstrate that Vitamin C is the most suitable reducing agent. Accordingly, all following studies utilized $FeSO_4$ and vitamin C only for iron (II) supplementation.

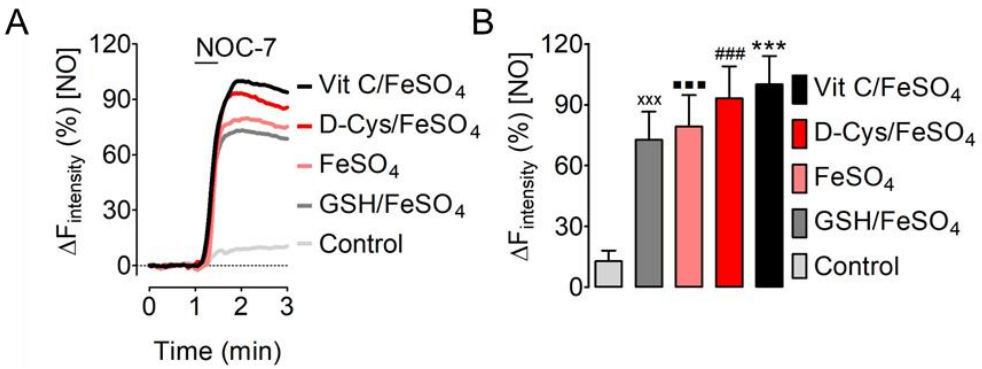

Figure 5.5. Vitamin C is one of the best-reducing agents for geNOps functionality. (A) Representative real-time traces of intracellular NO signals in response to 10 µM NOC-7 of HEK293T cells transiently expressing O-geNOp-NES. Cells have been treated with 1 mM of $FeSO_4$ supplemented with various reducing agents 1 mM GSH (dark grey curve), 1 mM D-Cysteine (red curve), 1 mM Vitamin C (black curve), and without any reducing agent (light pink curve). The control curve represents non-treated cells (light grey curve). (B) This panel presents the statistical analysis of the maximum response obtained from control (light grey bar, n=3/67), GSH (dark grey curve, n=3/57), only $FeSO_4$ (pink bar, n=3/74), D-Cysteine (red bar, n=3/78), and Vitamin C (black bar, n=3/91). Dunnett's Multiple Comparison Test was applied to compare all columns to the control column. All values are given as ±SD of at least 3 measurements. P-value summary: *p<0.0001*. (Control vs 1 mM GSH + 1 mM $FeSO_4$ ^{xxx}, Control vs 1 mM $FeSO_4$ ▪▪▪, Control vs 1 mM D-Cysteine + 1 mM $FeSO_4$ $^{###}$, Control vs 1 mM Vitamin C + 1 mM $FeSO_4$ ***).

5.2. Cell culture media with or without extra supplementation of Fe^{2+} and/or Vitamin C is insufficient for geNOps functionality

There are many conventional cell culture media containing different ferrous and ferric iron sources. In the next step, we investigated the effect of different iron forms and/or additives contained in 4 different commercial cell culture media on geNOps functionality (**Table 5.1**).

Table 5.1. Components of various conventional cell culture media

Medium	Component	Concentration (mg/L)	Additives (mg/L)
DMEM	Iron (III) Nitrate ($Fe(NO_3)_3$ x $9H_2O$)	0.10	-
Advanced DMEM	Iron (III) Nitrate ($Fe(NO_3)_3x9H_2O$); Iron (II) Sulfate ($FeSO_4$ x $7H_2O$)	0.05, 0.417	Ascorbic Acid Phosphate (2.5), Human Transferrin (7.5)
Ham's F12	Iron (II) Sulfate ($FeSO_4$ x $7H_2O$)	0.834	-
Ham's F12K	Iron (II) Sulfate ($FeSO_4$ x $7H_2O$)	0.8	-

One of the most common cell culture media is Dulbecco's Minimal Essential Media (DMEM) and as seen in **Figure 5.6A**, short-term (24 h) incubation of cells in these media is insufficient without any additional $FeSO_4$/Vitamin C treatment for the activation of geNOps. We observed the same result for Advanced DMEM (**Figure 5.6B**), Ham's F12 (**Figure 5.6C**), and Ham's F12K (**Figure 5.6D**). Although the administration of only Vitamin C as a reducing agent to the same media helped to reduce the iron compounds they contain, the desired functionality could not be observed in geNOps in short-term treatment (**Figure 5.6A-D**). Only $FeSO_4$ incubation with these 4 different media resulted in a significant increase in response compared to the control (**Figure 5.6A-D**). However, the addition of Vitamin C in addition to $FeSO_4$ in all 4 media resulted in the full functionality of geNOps (**Figure 5.6A-D**).

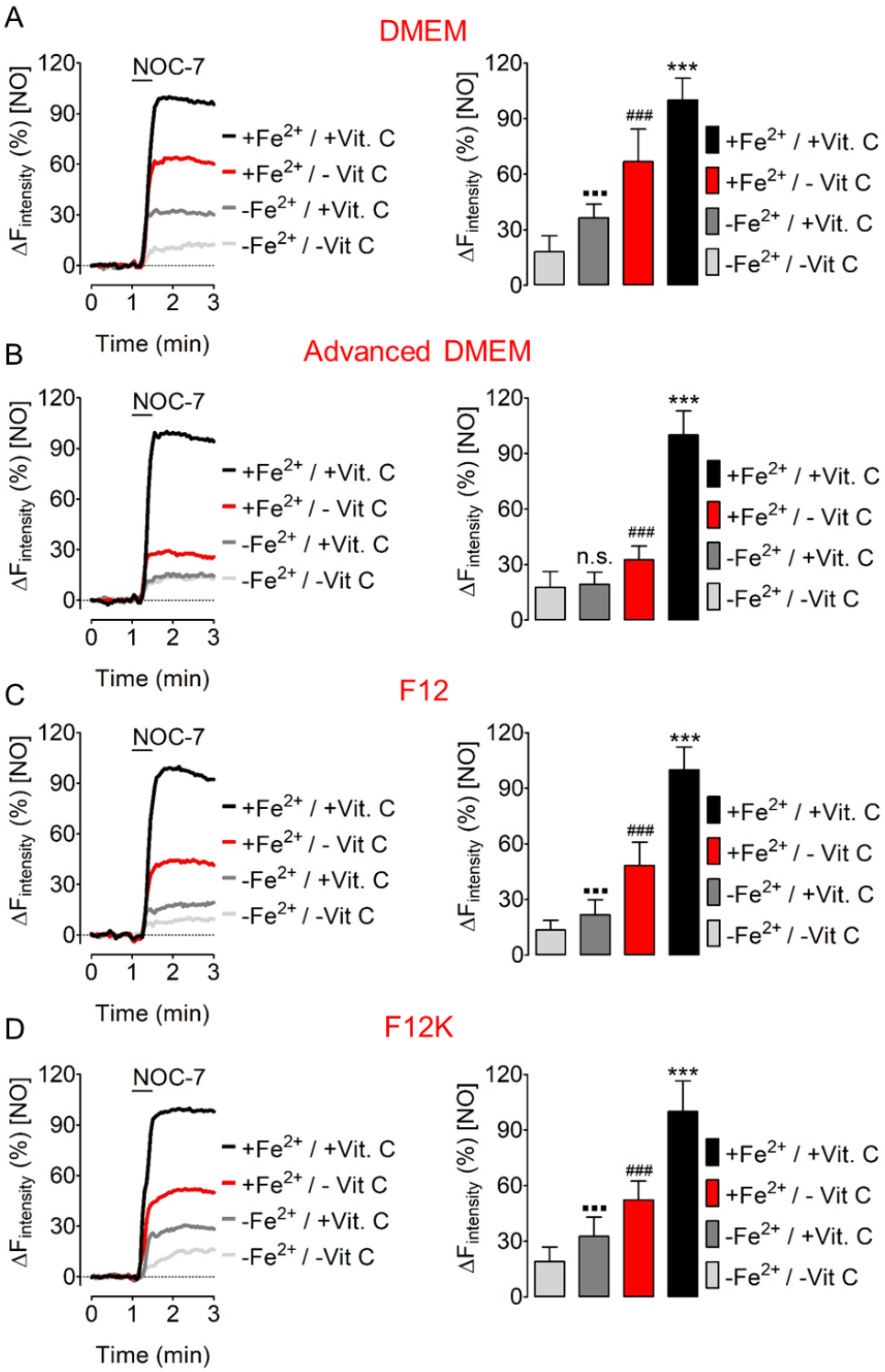

Figure 5.6. Conventional cell culture media containing different ferrous and/or ferric iron with other supplementations are not sufficient for geNOps functionality upon short-term treatment. This figure shows representative real-time NO traces of HEK293T cells expressing O-geNOp-NES. Light grey curves show NO signals under control conditions (no pre-treatment), dark grey curves upon 1 mM Vitamin C treatment, red curves show cells exposed to 1 mM $FeSO_4$, and black curves show NO responses to treatment with 1 mM $FeSO_4$ + 1 mM Vitamin C. All pretreatment procedures were conducted for 20 minutes before the imaging experiment. Under all experimental conditions, cells were cultured for 24 h in the respective media as indicated above each

panel. (A) Cells were cultured 24 h in Dulbecco's minimal essential medium (DMEM). Control conditions (no treatment, light grey curve and bar, n=3/42), pretreatment with 1 mM Vitamin C (dark grey curve and bar, n=3/55), with 1 mM $FeSO_4$ (red curve and bar, n=3/78), with 1 mM $FeSO_4$ + 1 mM Vitamin C (black curve and bar, n=3/90). (B) Same experimental setup as shown in panel A, except culturing of cells in Advanced DMEM. No treatment (light grey curve and bar, n=3/52), 1 mM Vitamin C (dark grey curve and bar, n=3/57), 1 mM $FeSO_4$ (red curve and bar, n=3/80), 1 mM $FeSO_4$ + 1 mM Vitamin C (black curve and bar, n=3/59). (C) Cells were cultured in Ham's F12 without any pretreatment (light grey curve and bar, n=3/74), 1 mM Vitamin C (dark grey curve and bar, n=3/72), 1 mM $FeSO_4$ (red curve and bar, n=3/123), 1 mM $FeSO_4$ + 1 mM Vitamin C (black curve and bar, n=3/125). (D) Cells were cultured in Ham's F12K after without any pretreatment (light grey curve and bar, n=3/49), 1 mM Vitamin C (dark grey curve and bar, n=3/56), 1 mM $FeSO_4$ (red curve and bar, n=3/53), 1 mM $FeSO_4$ + 1 mM Vitamin C (black curve and bar, n=3/34). Dunnett's Multiple Comparison Test was applied to compare all columns with the control column. All values denote mean ± SD., P-value summary: *p<0.0001*. (Control vs -Fe^{2+}/+Vit C■■■, Control vs +Fe^{2+}/-Vit C ###, Control vs +Fe^{2+}/+Vit C***).

Then, an experiment was repeated in parallel with short-term treatment, providing long-term treatment (21 days) of cells in these 4 different media. The aim here was to observe the NO response changes that occur in different conditions after the activity of geNOps is exposed to the iron concentration in the media for a long time. However, after the adaptation of the cells to the media, it did not produce an effective response on the iron metalloproteins in the media under control conditions (**Figure 5.7A-D**). Again, little change, which is not effective in NO responses, was observed in the case of only Vitamin C treatment. Interestingly, long-term treatment of only $FeSO_4$ did not show as a high response as short-term adapted cells although there was a significant difference (**Figure 5.7A-D**). And again, it was observed that $FeSO_4$/Vitamin C solution given acutely in all different media was more effective for the functionality of metalloprotein (**Figure 5.7A-D**). These results, obtained as a result of short-term and long-term treatments of different media, emphasized the iron (II) inadequacy of commercially available cell culture media and the necessity of acute ferrous iron and vitamin C treatment for metalloprotein functionality.

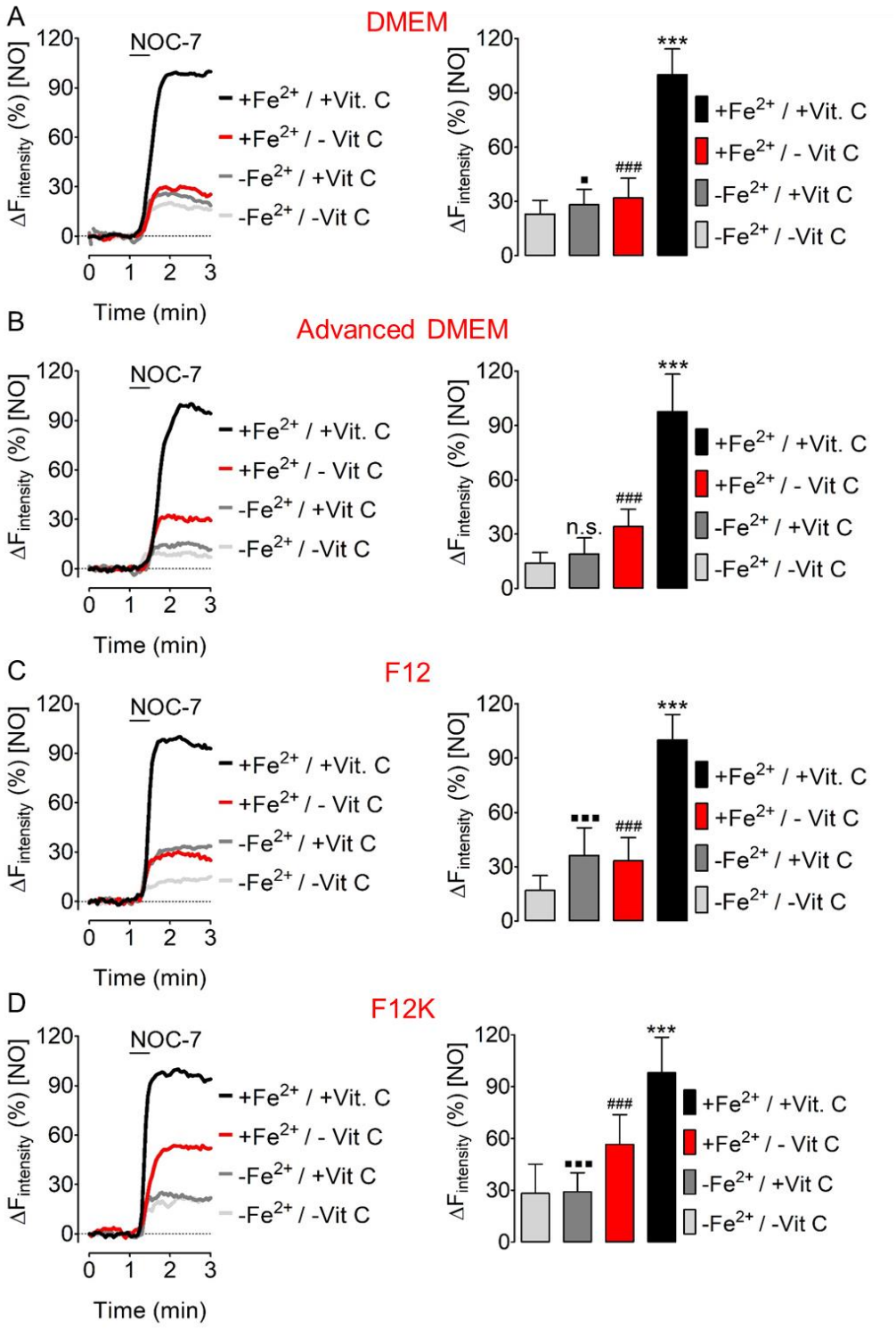

Figure 5.7. Same media are also insufficient for geNOps functionality upon long-term treatment. This figure shows representative real-time NO traces of HEK293T cells expressing O-geNOp-NES. Light grey curves show NO signals under control conditions (no pretreatment), dark grey curves upon 1 mM Vitamin C treatment, red curves show cells exposed to 1 mM $FeSO_4$, and black curves show NO responses upon treatment with 1 mM $FeSO_4$ + 1 mM Vitamin C. All pretreatment procedures were conducted for 20 minutes before the imaging experiment. Under all experimental conditions, cells were

cultured for 21 days in the respective media as indicated above each panel. (**A)** Cells were cultured for 21 days in Dulbecco's minimal essential medium (DMEM). Control conditions (no treatment, light grey curve and bar, n=3/88), pretreatment with 1 mM Vitamin C (dark grey curve and bar, n=3/60), with 1 mM $FeSO_4$ (red curve and bar, n=3/78), with 1 mM $FeSO_4$ + 1 mM Vitamin C (black curve and bar, n=3/89). (**B)** Same experimental setup as shown in panel A, except culturing of cells in Advanced DMEM. No treatment (light grey curve and bar, n=3/76), 1 mM Vitamin C (dark grey curve and bar, n=3/52), 1 mM $FeSO_4$ (red curve and bar, n=3/58), 1 mM $FeSO_4$ + 1 mM Vitamin C (black curve and bar, n=3/60). (**C)** Cells were cultured in Ham's F12 without any pretreatment (light grey curve and bar, n=3/32), 1 mM Vitamin C (dark grey curve and bar, n=3/28), 1 mM $FeSO_4$ (red curve and bar, n=3/31), 1 mM $FeSO_4$ + 1 mM Vitamin C (black curve and bar, n=3/45). (**D)** Cells were cultured in Ham's F12K after without any pretreatment (light grey curve and bar, n=3/64), 1 mM Vitamin C (dark grey curve and bar, n=3/67), 1 mM $FeSO_4$ (red curve and bar, n=3/81), 1 mM $FeSO_4$ + 1 mM Vitamin C (black curve and bar, n=3/69). Dunnett's Multiple Comparison Test was applied to compare all columns to the control column. All values denote mean ± SD, P-value summary: *p<0.0001*. (Control vs -Fe^{2+}/+Vit C▪▪▪, Control vs +Fe^{2+}/-Vit C $^{###}$, Control vs +Fe^{2+}/+Vit C***).

As a solution to the insufficient iron concentration of cell culture media, we added different concentrations of $FeSO_4$ or Vitamin C, separately, to these media for a long time. The effect of these indicated conditions on metalloprotein functionality after exposure of cultured cells was observed. **Figure 5.8A** and **Figure 5.8B** show cells exposed to different concentrations of $FeSO_4$ and Vitamin C for 1 day. We observed that HEK293T cells, which were treated with Vitamin C or $FeSO_4$ for a long time, deceased in the media containing high concentrations of Vitamin C or $FeSO_4$ (256 mg/L, 512 mg/L, and 1024 mg/L) deceased (**Figure 5.8A, B**). Cells were grown during 14 days in these stated concentrations of $FeSO_4$ and Vitamin C. In both conditions, the geNOps functionality was tested for 4 concentrations (2-4-8-16 mg/L) that allowed cells to survive after this prolonged incubation. Barely, no significant difference was observed in either condition compared to the control (**Figure 5.8C, D**). We didn't observe any change in cell morphology in cells long-term incubated at these different concentrations compared to control however, as seen, it was not sufficient for the activity of geNOps (**Figure 5.8C, D**). Also, no significant difference was observed between these concentrations compared to control (**Figure 5.8C, D**).

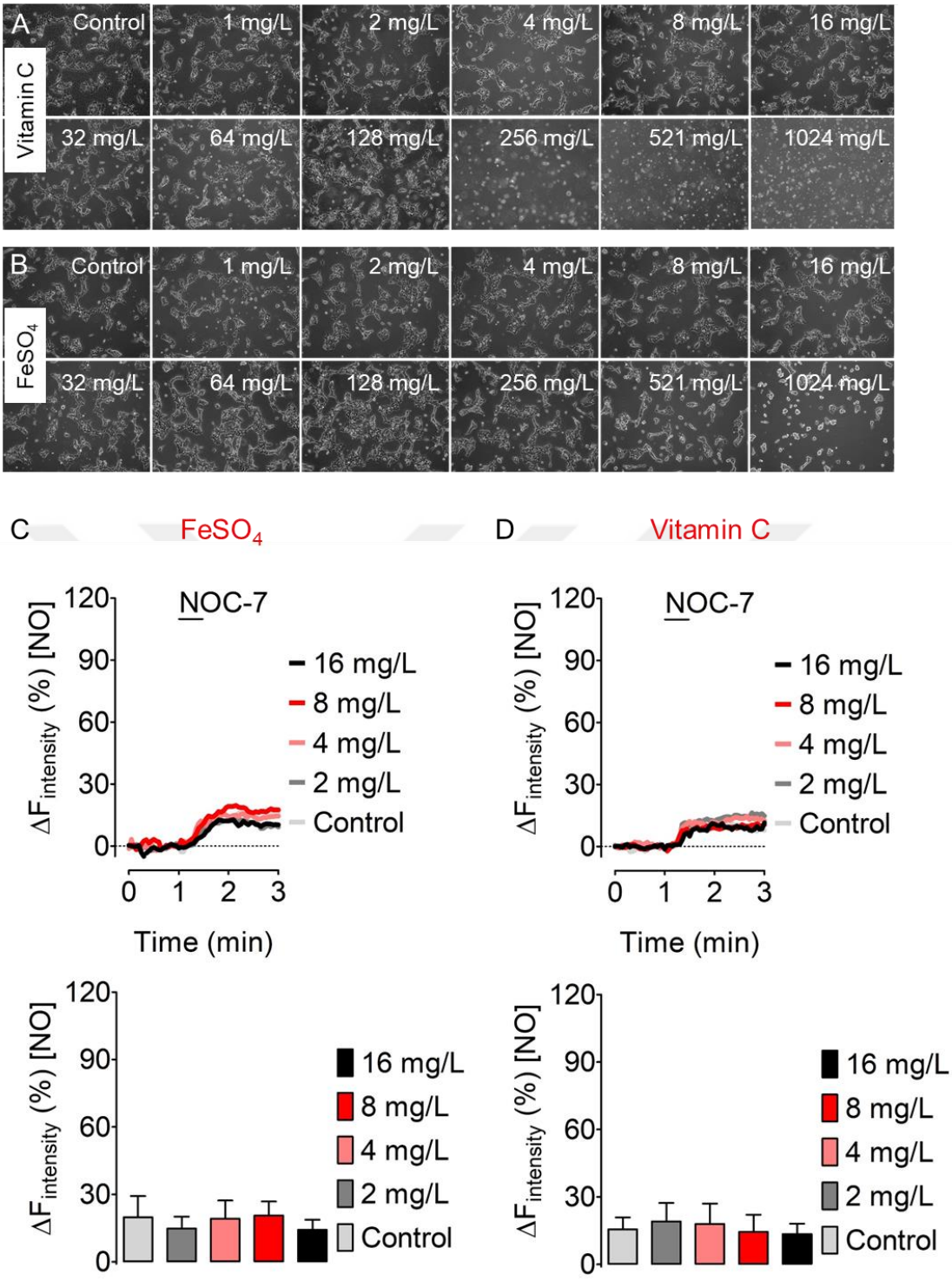

Figure 5.8. Cell culture media containing extra additional different concentrations of $FeSO_4$, or Vitamin C are not effective for geNOps functionality. (**A**) Representative bright-field images of HEK293T cells expressing O-geNOp-NES treated in different concentrations of Vitamin C. (**B**) Representative bright-field images of HEK293T cells expressing O-geNOp-NES treated in different concentrations of $FeSO_4$. (**C**) The curves in this panel show the average NO response of cells to 10 µM NOC-7 after long-term treatment of 0 mg/L (light grey curve), 2 mg/L (dark grey curve), 4 mg/L (pink curve), 8 mg/L (red curve), and 16 mg/L (black curve) $FeSO_4$ concentrations. Bar graph shows the statistical analysis of maximum NO response of cells in control (light grey bar, n=3/60),

2 mg/L (dark grey bar, n=3/65), 4 mg/L (pink bar, n=3/27), 8 mg/L (red bar, n=2/18), and 16 mg/L (black bar, n=3/21) $FeSO_4$ concentrations. (**D**) The curves in this panel show the average NO response of cells to 10 µM NOC-7 after long-term treatment of 0 mg/L (light grey curve), 2 mg/L (dark grey curve), 4 mg/L (pink curve), 8 mg/L (red curve), and 16 mg/L (black curve) Vitamin C concentrations. Bar graph shows the statistical analysis of maximum NO response of cells in control (light grey bar, n=3/74), 2 mg/L (dark grey bar, n=3/106), 4 mg/L (pink bar, n=3/111), 8 mg/L (red bar, n=2/113), and 16 mg/L (black bar, n=2/46) Vitamin C concentrations. Under all experimental conditions, cells were cultured for 14 days in the specified $FeSO_4$ or Vitamin C concentrations as above each panel. Dunnett's Multiple Comparison Test was applied to compare all columns to the control column. All values are given as ±SD. P-value summary: *p<0.0001*.

As a last experiment for this section, we observed NO responses by combining the highest concentration of $FeSO_4$ and Vitamin C from the previous experiment. We did not observe any morphological change in incubated cells with this combination at the end of 3 days (**Figure 5.9A**). As expected, the combination of sub-toxic concentrations of $FeSO_4$ (16 mg/L) and Vitamin C (8 mg/L) also failed to activate geNOps (**Figure 5.9B**). However, after cells adapted to $FeSO_4$ (16 mg/L) and Vitamin C (8 mg/L), they were acutely treated for 20 minutes with 1 mM $FeSO_4$, and 1 mM Vitamin C. As a result, geNOps displayed the massive functionality compared to control conditions and showed significant difference (**Figure 5.9B, C**). Overall, these data demonstrate that the geNOps functionality requires acute iron (II) treatment under standard cell culture conditions and extra additional ferrous iron and/or vitamin C are insufficient for geNOps functionality because of the oxidation of ferrous iron under the cell culture conditions.

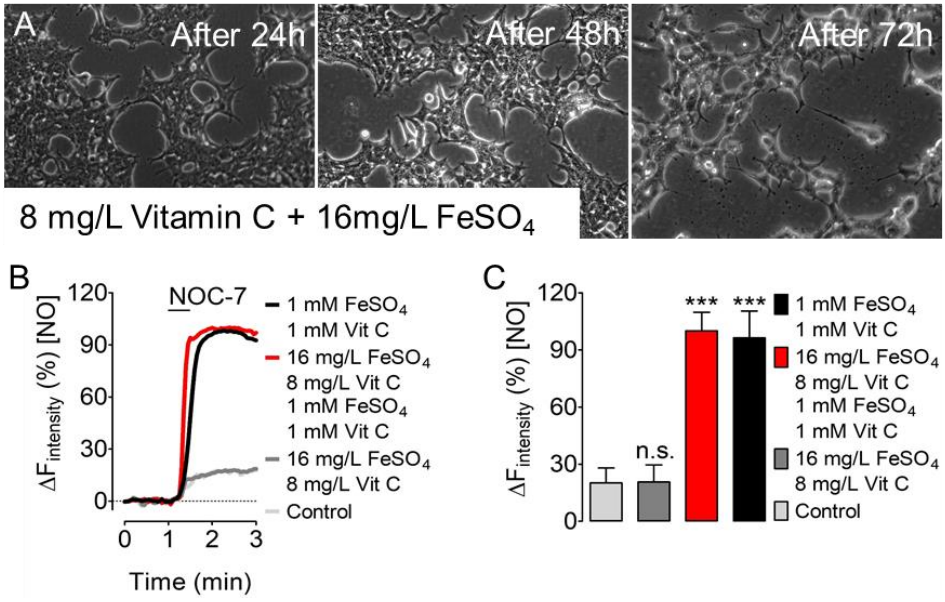

Figure 5.9. 16 mg/L FeSO4 and 8 mg/L Vitamin C does not activate geNOps

although acute supplementation does. (A) Representative bright-field images of HEK293T cells expressing O-geNOp-NES exposed to 16 mg/L $FeSO_4$ + 8 mg/L Vitamin C for 3 days. **(B)** The curves in this panel show the average O-geNOp-NES responses of HEK293T cells expressing upon administration of 10 µM NOC-7 with no treatment (light grey curve), with the treatment of 16 mg/L $FeSO_4$ and 8 mg/L Vitamin C (dark grey curve), upon acute treatment with 1 mM $FeSO_4$ + 1 mM Vitamin C for 20 minutes of cells that have been exposed to 16 mg/L $FeSO_4$ + 8 mg/L Vitamin C for 3 days (red curve), and control iron (II) treatment using 1 mM $FeSO_4$ + 1 mM Vitamin C to cells that were cultured in regular DMEM without long-term exposure to iron (black curve). **(C)** The bar graph shows the statistical analysis of maximum NO response of cells as indicated in panel B. Light grey bar indicates the maximum response of cells without any treatment (n=3/63), dark grey bar shows the maximum response of cells treated with 16 mg/L $FeSO_4$ + 8 mg/L Vitamin C for 3 days (n=3/18), red bar represents the maximum response of cells, which were incubated 16 mg/L $FeSO_4$ + 8 mg/L Vitamin C with an additional 1 mM $FeSO_4$ + 1 mM Vitamin C for 20 minutes treatment (n=3/27), and black bars show the maximum response of cells treated with 1 mM $FeSO_4$ + 1 mM Vitamin C (n=3/48). Dunnett's Multiple Comparison Test was applied to compare all columns to the control column. All values are given as ±SD. P-value summary: $p<0.0001$, ***.

5.3. Imaging of intracellular Fe^{2+}/Fe^{3+} distribution in cultured cells

Studies so far have demonstrated the requirement for iron (II) for geNOps to function in cultured cells. As a further study, we aimed to correlate these results with FeRhoNox-1, one of the probes used to detect intracellular labile ferrous iron. We performed high-resolution confocal imaging experiments using this probe in different treatment conditions. Co-staining HEK293T cells with Hoechst and FeRhoNox-1 unveiled that the Fe^{2+} specific probe localizes mainly around the nuclear membrane, the Golgi apparatus, and undefinable intracellular structures and vesicles (**Figure 5.10A**). However, the FeRhoNox-1 probe displayed detectable changes in fluorescence under control conditions, without any treatment. Cell treatment with Vitamin C, $FeSO_4$, and the combination of $FeSO_4$ and Vitamin C caused a continuously increasing intracellular fluorescence signal indicating the uptake and accumulation of reduced and labile iron (II) in these cells (**Figure 5.10B)** The FeRhoNox-1 results are in line with geNOps responses (**Figure 5.10C**). These results support our first goal, that geNOps are suitable for indirect ferrous iron detection, and once again demonstrated the necessity of iron (II) for metalloprotein functionality.

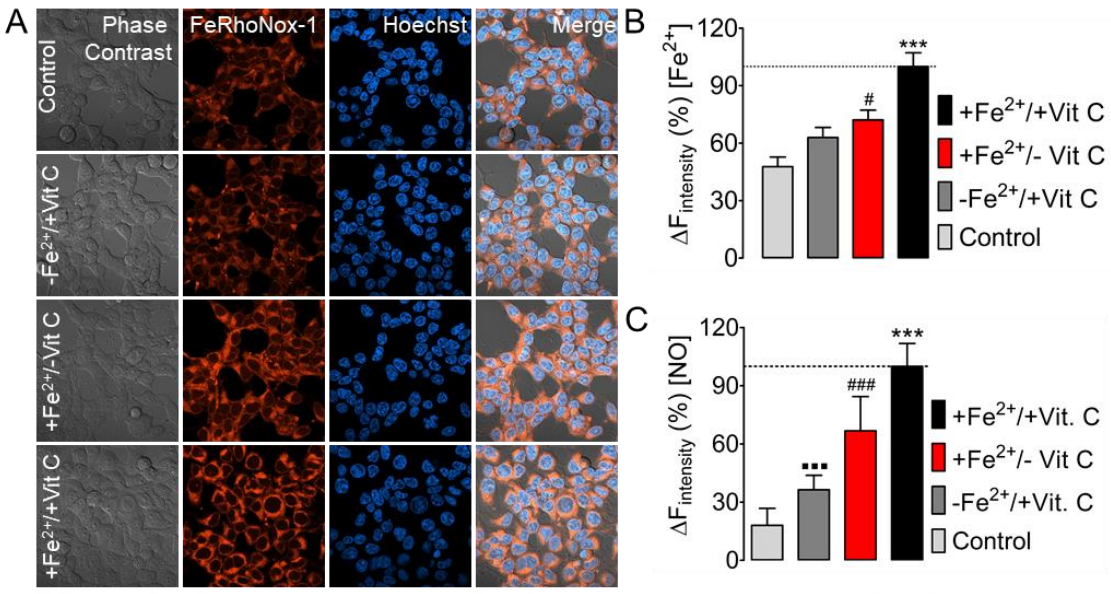

Figure 5.10. Visualizing the Fe^{2+} content in live cells with the aid of FeRhoNox-1. (A) Representative high-resolution confocal images of HEK293T cells co-stained with FeRhoNox-1 and Hoechst, respectively. Upper panel images show untreated cells, second-line images show cells treated with 1 mM Vitamin C, third line shows images of cells pre-treated with 1 mM $FeSO_4$, and images on the bottom show cells pre-treated with 1 mM $FeSO_4$ and 1 mM Vitamin C. All treatment times are 20 min. (B) Bars denote analysis of the images represented in panel A. Light grey bars represent non-treated cells (n=2/7), dark grey bars show cells treated with 1 mM Vitamin C (n=3/9), red bars show cells exposed to 1 mM $FeSO_4$ (n=3/10), and black bars show cell treatment with 1 mM $FeSO_4$ + 1 mM Vitamin C (n=3/11). (C) Bars indicate the maximum response of NO in control conditions (light grey bar, n=3/42), or pretreatment with 1 mM Vitamin C (dark grey bar, n=3/55), or with 1 mM $FeSO_4$ (red bar, n=3/78), or with 1 mM $FeSO_4$ + 1 mM Vitamin C (black bar, n=3/90). Dunnett's Multiple Comparison Test was applied to compare all columns with the control column. All values denote mean ± SD, P-value summary: *$p<0.0001$*. (Control vs -Fe^{2+}/-Vit C▪▪▪, Control vs +Fe^{2+}/-Vit C $^{\#}$, Control vs +Fe^{2+}/+Vit C***).

We again utilized the FeRhoNox-1 probe and collected multiple focal planes in the Z-direction using high-resolution confocal microscopy to localize intracellular labile iron. From the top to the bottom, this approach, however, unveiled that ferrous iron or the dye itself accumulated on the cell surface primarily (**Figure 5.11A-D**). Overall, these experiments demonstrate once again that well-established iron (II) detection probes bear severe caveats in the detection and localization of intracellular labile iron.

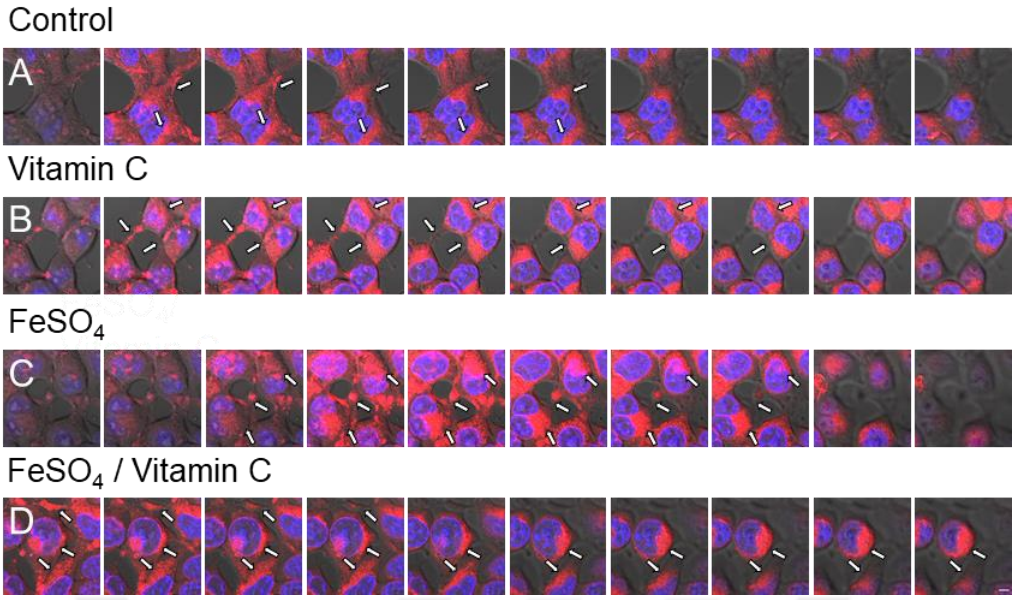

Figure 5.11. Z-stack images of HEK293T cells using a high-resolution confocal microscope. High-resolution confocal images of HEK293T cells with no treatment (**Panel A**) or pre-treated with 1 mm Vitamin C (**Panel B**) or pre-treated with 1 mM $FeSO_4$ (**Panel C**) or pre-treated with 1 mM $FeSO_4$ + 1 mM Vitamin C (**Panel D**) co-stained with FeRhoNox-1 and Hoechst. All treatments were carried out for 20 minutes.

To further confirm these observations, whether iron accumulates on the cell surface or not, we next imaged cells stained with the Perls/DAB (3'-diaminobenzidine) method. Cells treated with Vitamin C only were similar to the control group (**Figure 5.12A, B**). However, $FeSO_4$ only treated cells displayed a remarkable accumulation of extracellular iron-particles, indicating that the majority of provided iron precipitates without entering the cells and aggregates on the surface of the cell membrane (**Figure 5.12A, B**). In addition, the treatment of solution containing both $FeSO_4$, and Vitamin C did not cause such clear accumulation (**Figure 5.12A, B**).

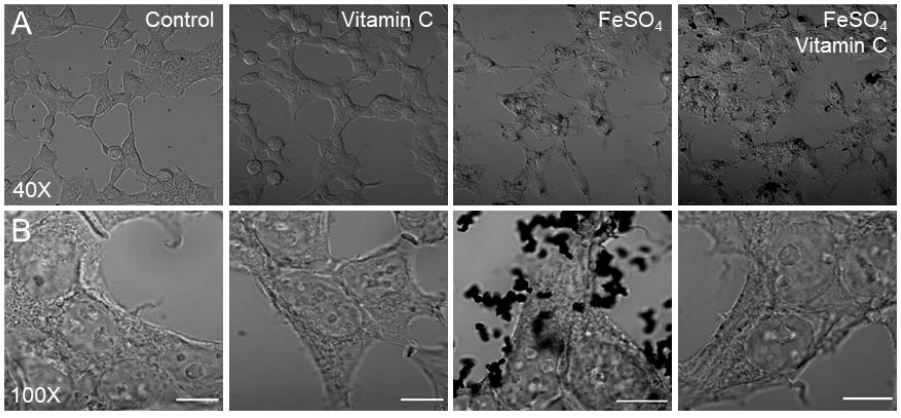

Figure 5.12. Perls/DAB staining to determine the iron distribution in HEK293T

cells. Phase-contrast images of Perls/DAB stained HEK293T cells under different conditions as control, Vitamin C, $FeSO_4$, and $FeSO_4$ + Vitamin C in using 40X objective (**Panel A**) and 100X objective (**Panel B**).

5.4. Optimization of the iron-provision procedure

So far, we have used high iron (II) and Vitamin C concentrations in our experiments and showed the accumulation of iron because of this concentration in the previous visualization experiments. Thus, we next sought to optimize the acute iron (II) provision procedure in normal cell culture conditions to reduce the amount of the reducing agent and iron compound by employing the design of experiments using the Taguchi approach. We have arranged and tested 3 parameters including $FeSO_4$ and Vitamin C concentration and incubation time, respectively, with the help of the Taguchi array shown in **Table 5.2**.

Table 5.2. Design of Experiment according to Taguchi Array

Experimental Run	$FeSO_4$ (µM)	Vitamin C (µM)	Incubation Time (min)	Response (%)
1	30	50	5	34,1
2	300	1000	5	74,9
3	1000	500	5	86,2
4	30	50	10	53,4
5	30	500	10	46,7
6	100	500	10	78,2
7	300	50	10	76,4
8	300	300	10	88,8
9	***1000***	***1000***	***10***	***100***
10	30	300	15	79,6
11	30	1000	15	46,3
12	100	50	15	61,7
13	***300***	***500***	***15***	***97,9***
14	1000	50	15	84
15	30	500	20	81,4
16	100	300	20	81,8
17	300	50	20	87,7

In cases where the amount of iron and Vitamin C is high, the low incubation period showed that we could not get a sufficient NO response (**Figure 5.13A**). It was also observed that NO responses decreased at high $FeSO_4$ and low Vitamin C concentrations (**Figure 5.13C**). The results of this approach yielded the minimum required concentration of the iron (II) compound and the reducing agent and the incubation time as 300 µM, 500 µM, and 15 minutes, respectively (**Figure 5.13A-D**).

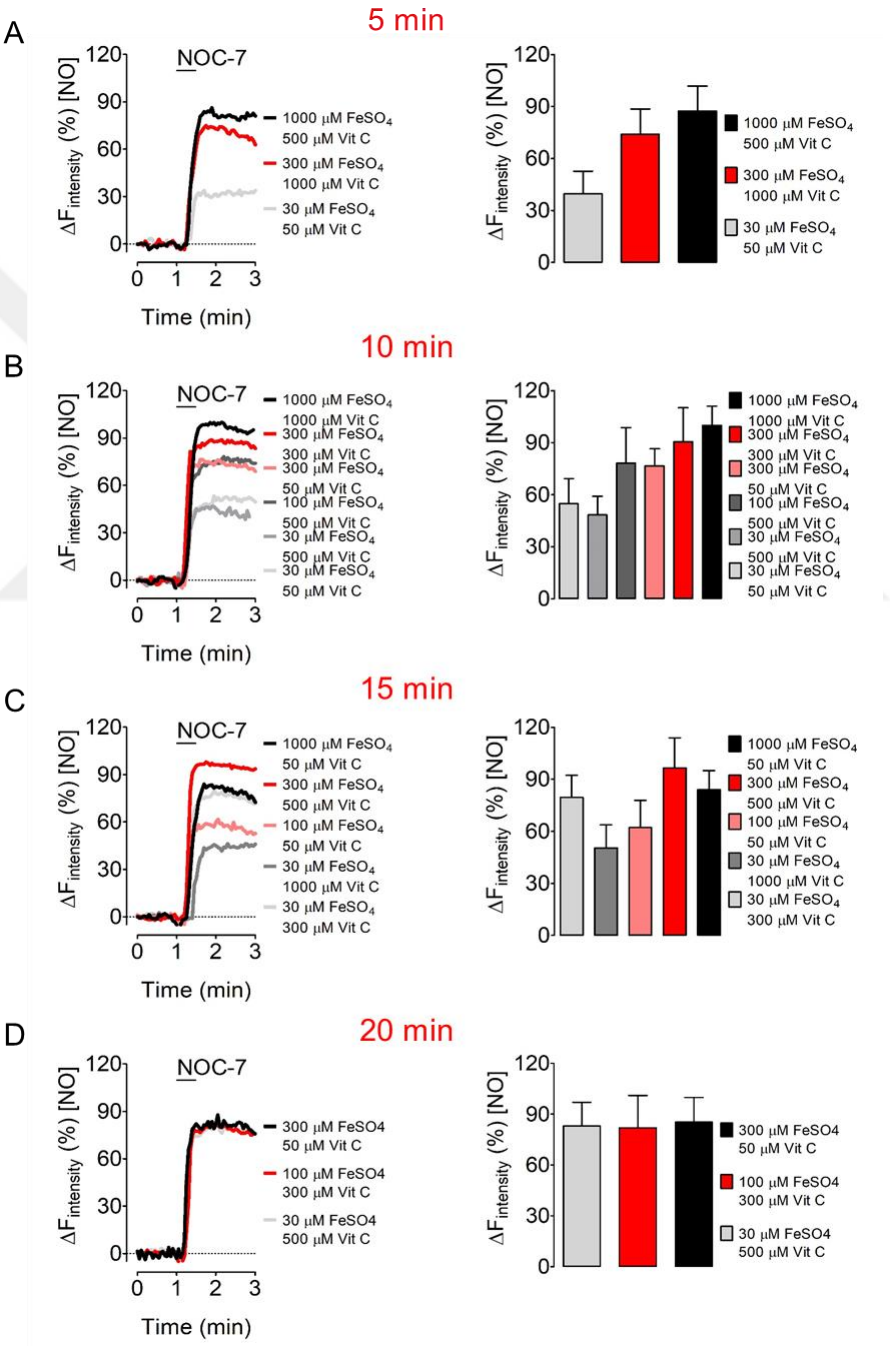

Figure 5.13. Design of experiment with Taguchi array to determine the optimum concentration of $FeSO_4$ and Vitamin C with incubation time. (A) Representative bars

show the average NO response of HEK293T cells expressing O-geNOp-NES in response to 10 µM NOC-7 after treatment of 5 minutes with 30 µM $FeSO_4$ + 50 µM Vitamin C (first orange bar, n=2/55), 300 µM $FeSO_4$ + 1000 µM Vitamin C (red curve or bar, n=58), 1000 µM $FeSO_4$ + 500 µM Vitamin C (black curve or bar, n=2/69). (B) Same experimental setup as in panel A but 10 minutes incubation time has been applied. 30 µM $FeSO_4$ + 50 µM Vitamin C (light grey curve or bar, n=2/62), 30 µM $FeSO_4$ + 500 µM Vitamin C (grey curve or bar, n=2/52), 100 µM $FeSO_4$ + 500 µM Vitamin C (dark grey curve or bar, n=2/59), 300 µM $FeSO_4$ + 50 µM Vitamin C (pink curve or bar, n=2/48), 300 µM $FeSO_4$ + 300 µM Vitamin C (red curve or bar, n=2/63), and 1000 µM $FeSO_4$ + 1000 µM Vitamin C (black curve or bar, n=2/61). (C) Same experimental setup as in panel A but 15 minutes incubation time has been applied. 30 µM $FeSO_4$ + 300 µM Vitamin C (light grey curve or bar, n=2/50), 30 µM $FeSO_4$ + 1000 µM Vitamin C (dark grey curve or bar, n=2/25), 100 µM $FeSO_4$ + 50 µM Vitamin C (pink curve or bar, n=2/62), 300 µM $FeSO_4$ + 500 µM Vitamin C (red curve or bar, n=2/105), 1000 µM $FeSO_4$ + 50 µM Vitamin C (black curve or bar, n=2/50). (D) Same experimental setup as in panel A but 20 minutes incubation time has been applied. 30 µM $FeSO_4$ + 500 µM Vitamin C (light grey curve or bar, n=2/48), 100 µM $FeSO_4$ + 300 µM Vitamin C (red curve or bar, n=2/54), and 300 µM $FeSO_4$ + 50 µM Vitamin C (black curve or bar, n=2/29). All values denote mean ±S.D.

In the next step, we compared the new iron solution obtained as a result of the Taguchi experiments with the standard iron solution for the control. As shown in **Figure 5.14A**, the optimized parameters yielded similar responses to exogenous NO compared to the standard iron (II) treatment and showed a significant difference with control like the standard iron (II) treatment (**Figure 5.14B**). Thus, we observed that the new iron solution is suitable for geNOps functionality. Furthermore, FeRhoNox-1 imaging experiments which we did to observe the distribution of iron in the cell, also confirmed these observations (**Figure 5.14C, D**). The optimized solution showed an observable iron content like the standard solution, with a significant difference compared to the control. After the FeRhoNox-1 experiment, it was shown that there was no cell surface accumulation in the Z-stacks of cells treated with optimized solution taken with the help of high-resolution confocal microscopy (**Figure 5.14E**). Overall, our data suggest that significantly lower $FeSO_4$ and Vitamin C concentrations are sufficient to activate the geNOps and this treatment did not cause the accumulation on the cell surface.

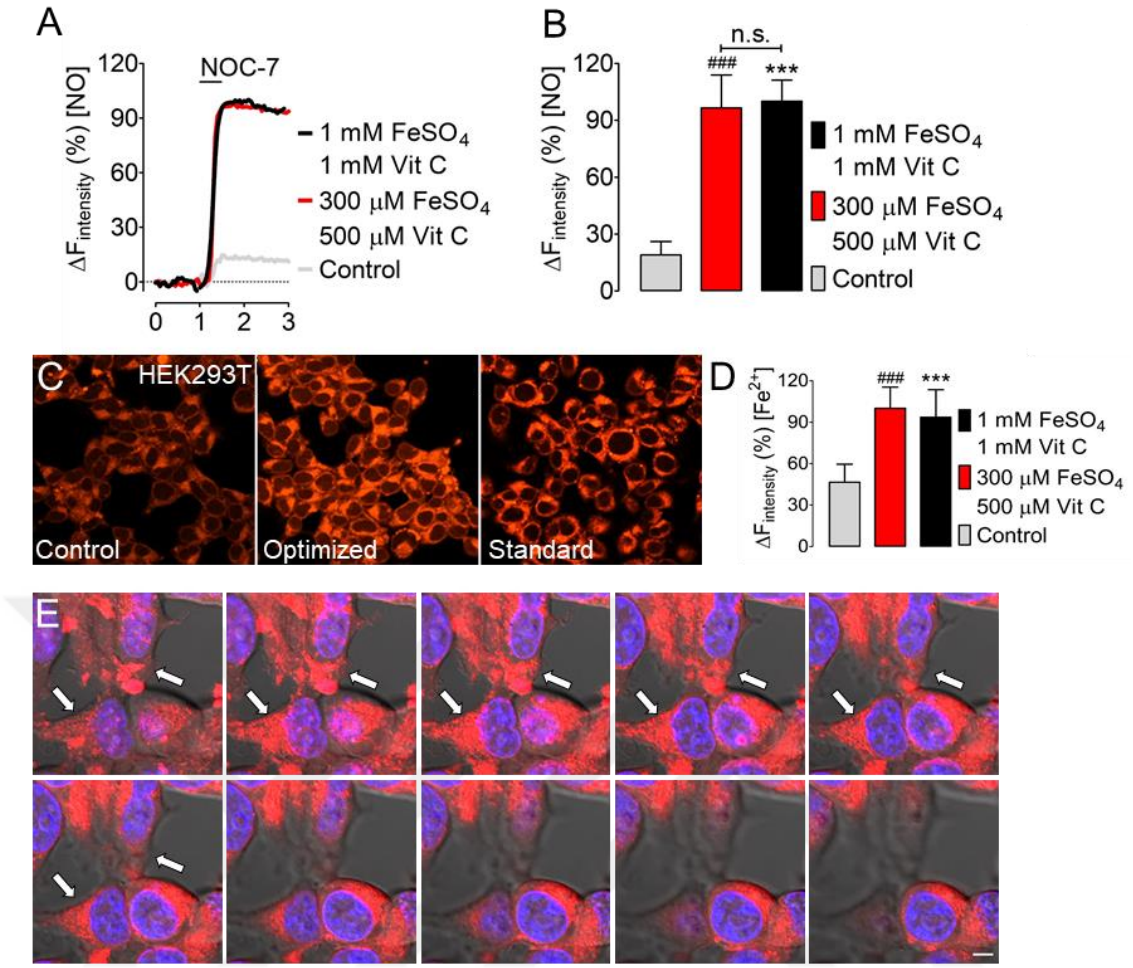

Figure 5.14. Optimization of the iron (II) loading procedure in cultured cells. (A) The upper panel shows representative real-time NO traces of signals in HEK293T cells expressing O-geNOp-NES in response to 10 µM NOC-7. Cells were pre-treated with 1 mM $FeSO_4$ + 1 mM Vitamin C for 20 min (black curve) or 300 µM $FeSO_4$ + 500 µM Vitamin C for 15 min (red curve) or without any treatment (light grey curve) before imaging experiment. **(B)** This panel shows a statistical analysis of maximum NO response to cell treatment with 10 µM NOC-7. The control bar represents cells without iron (II) treatment (light grey bar, n=3/36), the red bar indicates cells that have been treated with 300 µM $FeSO_4$ + 500 µM Vitamin C (n=3/48), and black bar represents cells treated with the standard solution comprising 1 mM $FeSO_4$ + 1 mM Vitamin C (n=3/53). **(C)** Representative confocal images of HEK293T cells co-stained with Hoechst and FeRhoNox-1 under non-treated conditions (left image indicated as control) and after treatment with 300 µM $FeSO_4$ + 500 µM Vitamin C for 15 minutes (middle image indicated as optimized), or 1 mM $FeSO_4$ + 1 mM Vitamin C for 20 min (right image indicated as standard). **(D)** Statistical analysis represents maximum FeRhoNox-1 intensities under normal conditions (grey bar, n=2/7), optimized iron (II) concentration conditions (red bar, n=2/10) or standard iron (II) treatment conditions (black bar, n=2/11). **(E)** Z-stacks images of HEK293T cells pre-treated with 300 µM $FeSO_4$ + 500 µM Vitamin C for 15 minutes using high-resolution confocal microscopes. Cells were co-stained with FeRhoNox-1 and Hoechst. Dunnett's Multiple Comparison Test was applied to compare all columns to the control column. All values denote mean ±SD. P-value summary: *p<0.0001*. (Control vs 300 µM $FeSO_4$ + 500 µM Vitamin C$^{###}$, Control vs 1 mM $FeSO_4$ + 1 mM Vitamin C***).

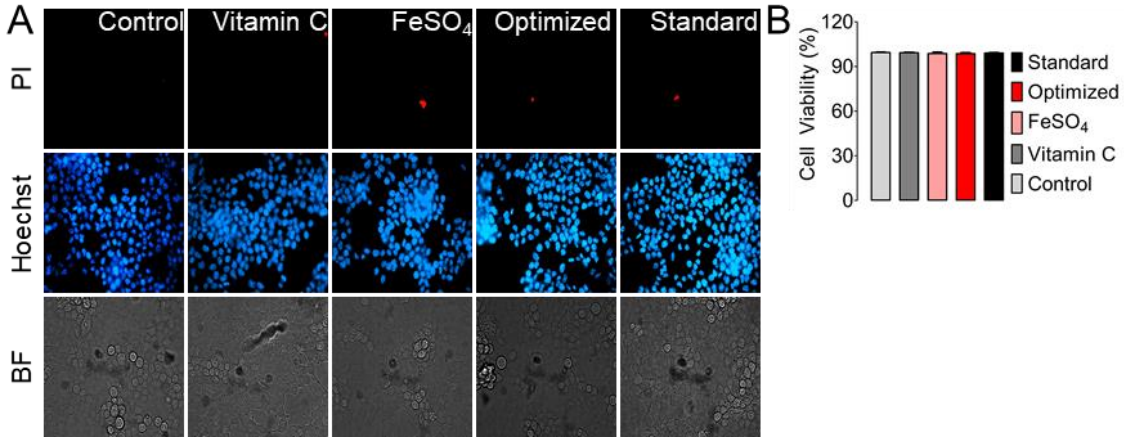

Figure 5.15. Apoptosis Assay upon treatment of iron (II) loading. (A) Representative wide-field images of HEK293T cells under control conditions (1st column), or 1 mM Vitamin C (2nd column), or 1 mM $FeSO_4$ (3rd column), or 300 µM $FeSO_4$ + 500 µM Vitamin C (4th column, optimized) 1 mM $FeSO_4$ +1 mM Vitamin C (5th column, standard). First raw shows representative wide-field images stained with Propidium Iodide (PI), the second raw shows the same cells dyed with Hoechst, and the last raw shows respective bright-field images. **(B)** The bars represent the statistical analysis of cell viability derived from the images shown in panel A. Statistical difference between the control group (grey bar, n=7/1864), Vitamin C (dark grey bar, n=7/1719), 1 mM $FeSO_4$ (pink bar, n=9/2131), 300 µM $FeSO_4$ + 500 µM Vitamin C (red bar, n=7/2010), and standard conditions 1 mM $FeSO_4$ + 1 mM Vitamin C (black bar, n=7/1854). Dunnett's Multiple Comparison Test was applied to compare all columns to the control column. All values denote mean ±SD. P-value summary: $p<0.05$.

The effect of iron supplementation on cell viability was tested by nuclear staining (Hoechst 33342) and PI using a newly optimized $FeSO_4$/Vitamin C solution along with all previously used conditions. As a result of this experiment, all conditions did not have a significant effect on cell viability in HEK293T cells compared to control (**Figure 5.15A, B**).

We next sought to test the optimized iron (II) solution in cells capable of producing intracellular NO. For this purpose, we utilized the immortalized human umbilical vein endothelial cells (EA. hy926). Because of the poor transfection efficiency, we generated a new EA. hy926 cell line expressing O-geNOp-NES using lentivirus approaches. As shown in **Figure 5.16A** high transfection efficiency was observed in these stable cell lines. Cells treated with optimized iron (II) solution caused a worthwhile intracellular NO signal in response to adenosine triphosphate (ATP), which activates the G-protein-coupled P2Y2 receptor in these cells, while the cells without iron treatment remained

silent (**Figure 5.16B**). Also, cells treated with the optimized iron solution before the imaging experiment showed a pivotal significant difference compared to control (**Figure 5.16C**). Treatment of cells with L-NAME which is an endothelial nitric oxide synthase inhibitor caused the decreasing of NO response as expected (**Figure 5.16B, C**). This result shows that the new iron solution we determined for the activation of geNOps is effective for observing endogenous NO changes as well as exogenous NO responses.

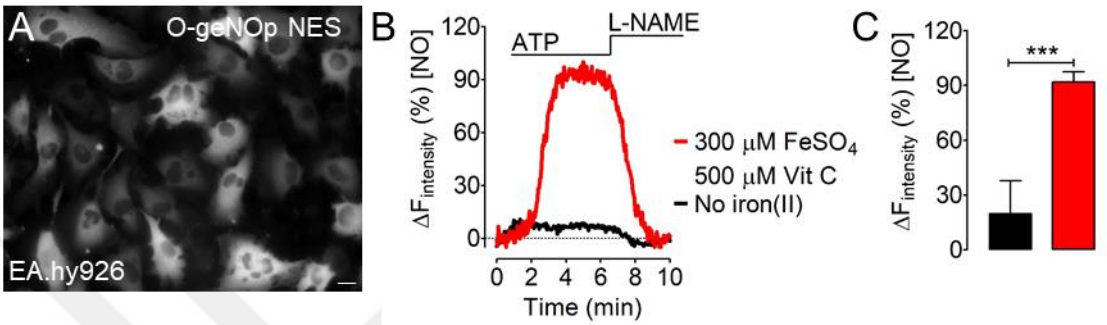

Figure 5.16. Endogenous NO response of EA. hy926 cells stably expressing O-geNOp-NES upon iron (II) treatment. (A) Representative wide-field images of EA. hy926 cells stably expressing O-geNOp-NES. **(B)** Representative real-time traces show endogenous NO responses of EA. hy926 cells adapted to 18 kPa O_2 prior to acute treatment with 100 µM ATP and subsequent administration of 500 µM L-NAME without any iron (II) treatment (black curve) or incubation of cells in 300 µM $FeSO_4$ + 500 µM Vitamin C (red curve). **(C)** Bars show the maximum NO response of EA. hy926 cells to 100 µM ATP (red bar, n=3/29) and to 10 µM NOC-7 (black curve, n=3/54) compared to basal levels (white bars). An unpaired t-test was applied for statistical analysis. All values denote mean ± SD. P-value summary: *$p<0.0001$,* ***.

As the last experiment of the study, we checked whether the iron we supplemented caused any oxidative stress in the cell. At this stage, we applied the co-culture method, a newly published method for stable EA. hy926 cells targeted different locales, and quantitatively measured the basal H_2O_2 level in 3 different conditions in different locales as the nucleus, mitochondria, and cytosol (*Secilmis et al.,2021*). As a result of this experiment, EA. hy926 cells treated with the optimized iron (II) solution did not show oxidative stress at any locales in the cell (**Fig. 5.17A, B**). For the same purpose, we observed the effect of iron on H_2O_2 in mitochondria of HEK293T transiently expressing Hyper7.2 targeted mitochondria. We did not any change in basal H_2O_2 in all conditions, especially in the optimized iron solution (**Figure 5.17C, D**).

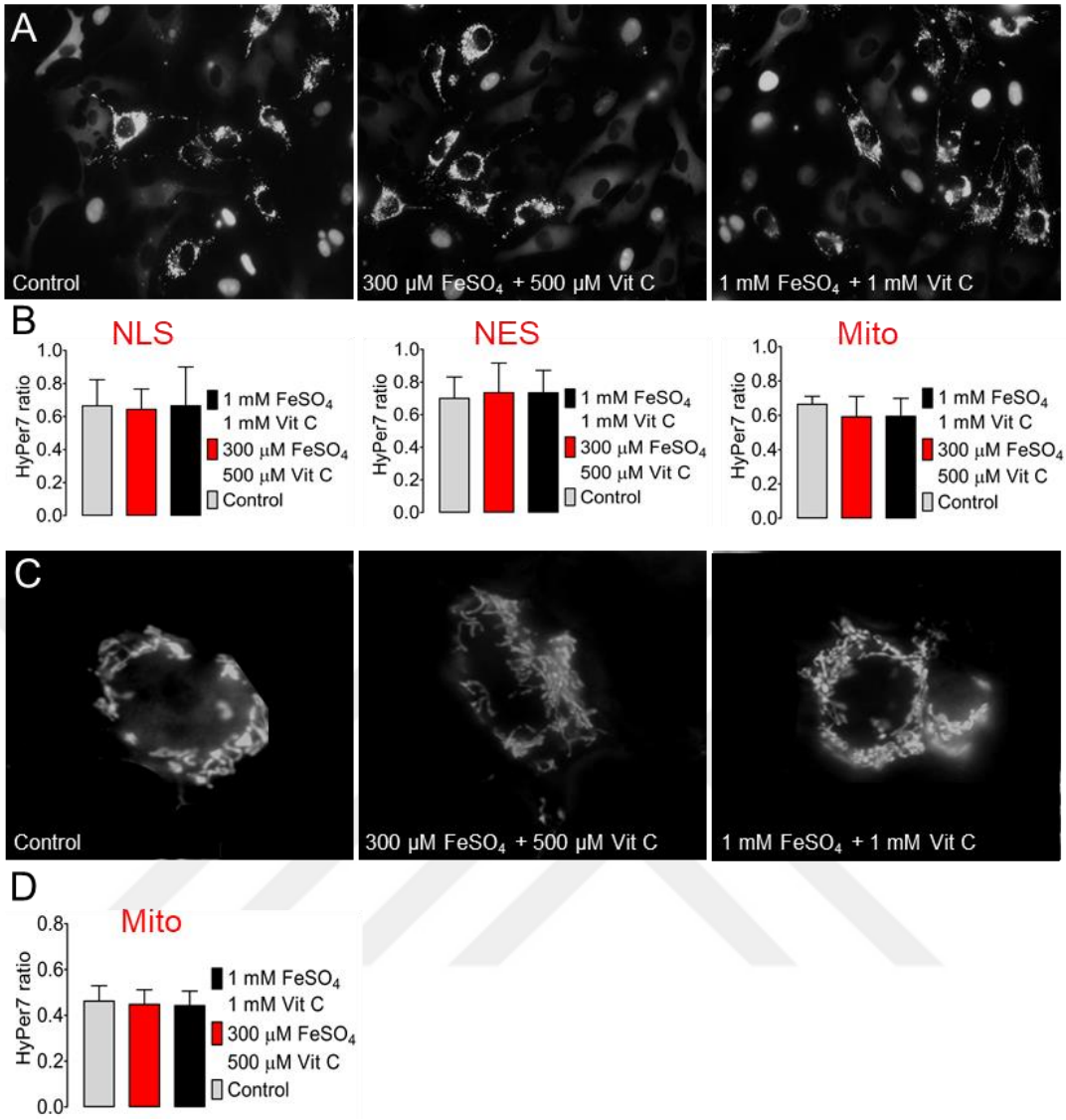

Figure 5.17. Optimized iron (II) loading does not cause oxidative stress in EA. Hy926 and HEK293T cells. (A) Representative wide-field images of co-cultured EA. hy926 cells stably expressing mitochondria, nucleus, and cytosol targeted HyPer7.2 without any treatment (left image) or pre-treated with 300 µM $FeSO_4$ + 500 µM Vitamin C (middle image) or pre-treated with 1 mM $FeSO_4$ + 1 mM Vitamin C (right image). **(B)** Statistical analysis of basal HyPer7.2 levels in the mitochondria, nucleus, and cytosol under control conditions (grey bars) and upon exposure to 300 µM $FeSO_4$ + 500 µM Vitamin C (red bars), or 1 mM $FeSO_4$ + 1 mM Vitamin C (black bars). Left bars show HyPer7.2 ratios in the nucleus (control, grey bars, n=22/152), in response to 15 minutes incubation with 300 µM $FeSO_4$ + 500 µM Vitamin C (red bars, n=30/139) and upon treatment with 1 mM $FeSO_4$ + 1 mM Vitamin C for 20 minutes (black bars, n=29/149). Middle bars show HyPer7.2 ratios in the cytosol (control, grey bars, n=22/65), in response to 15 minutes incubation with 300 µM $FeSO_4$ + 500 µM Vitamin C (red bars, n=30/104) and upon treatment with 1 mM $FeSO_4$ + 1 mM Vitamin C for 20 minutes (black bars, n=29/99). The bars on the right show HyPer7.2 ratios in the mitochondria (control, grey bars, n=22/137), in response to 15 minutes incubation with 300 µM $FeSO_4$ + 500 µM Vitamin C (red bars, n=30/153) and upon treatment with 1 mM $FeSO_4$ + 1 mM Vitamin C for 20 minutes (black bars, n=29/148). **(C)** Representative wide-field images of HEK293T

expressing mitochondria-targeted HyPer7.2 without any treatment (left image) or pre-treated with 300 μM $FeSO_4$ + 500 μM Vitamin C (middle image) or pre-treated with 1 mM $FeSO_4$ + 1 mM Vitamin C (right image). **(D)** The bar shows the statistical analysis of basal H2O2 levels in mitochondria via HyPer7.2 control conditions (grey bar, n=20/153) and upon exposure to 300 μM $FeSO_4$ + 500 μM Vitamin C for 5 minutes (red bar, n=17/160), or 1 mM $FeSO_4$ + 1 mM Vitamin C for 20 minutes (black bar, n=19/155). Different targeted Hyper7.2 was excited at 420 nm and 499 nm and emission was collected at 516 nm. Dunnett's Multiple Comparison Test was applied to compare all columns to the control column. All values denote mean ±SD. P-value summary: $p<0.05$.

6. DISCUSSION

In this present study, we conducted research to present genetically encoded nitric oxide probes as a model system aiming to observe the behavior of iron-dependent metalloproteins indirectly under cell culture conditions. The geNOps contain a GAF domain, as NO detection region, and fluorescent protein (*Eroglu et al., 2016*). In addition, NO specific GAF domain has a non-heme ferrous iron center and NO binds to this center. Based on this, we completed our work in 4 objectives.

In the first step, we observed the difference in the response of the biosensor we used in our study in the presence and absence of iron. geNOps activity, which was not excessive in the absence of iron, improved in the presence of iron (Figure 5.1). This proved that the geNOps model we presented in this study can be an indirect reporter for iron and that iron is required for its activation. In a study by Gao and O'Brian, they observed that the low expression of iron-dependent cytochrome c1 in the bacterial strain in case of the iron limitation (*Gao & O'Brian, 2005*). When they added supplementation media containing heme iron, they observed high expression of cytochrome c1 protein. This, in line with our work, highlights the necessity of iron for the activation of iron-dependent metalloprotein.

Since the development of geNOps, a standard solution has been used using iron (II) fumarate, which is a poorly water-soluble ferrous iron compound, and Vitamin C (*Eroglu et al., 2016*). Although this iron solution used was effective for the function of geNOps, it had some limitations. One of these was the mechanical mixing step, which must be done to ensure that the ferrous fumarate can be dissolved in the physiologic buffer. The solubility of iron (II) fumarate in water at room temperature is small (*Kapor et al., 2012*) and under normal conditions, iron compounds are easier to dissolve in acidic solutions (*Aslamkhan et al., 2002; Garcia Casal et al., 2001*). However, since the physiological buffer solutions used during the experiments are neutral, the prepared solution using only

iron will precipitate after a while, even if it is dissolved with a mechanical stirrer for a certain period. We demonstrated this required mixing time with the help of ferrozine in this study (Figure 5.2). Ferrozine is an indicator compound for iron and is used as a colorimetric assay used for the determination of ferrous iron in solution by forming a complex (*Carpenter & Ward, 2017*). In conclusion, we showed that mechanical mixing for at least 2 hours is required if ferrous (II) fumarate is used as the iron source required for the activation of geNOps. This was a pivotal factor limiting the usage of geNOps.

After deciding that geNOps would not work without iron supplementation and that iron (II) fumarate required a long dissolution period, the first step was to search for another source of ferrous iron instead of iron (II) fumarate that would both activate geNOps and be used immediately after adding it to the physiological buffer. For this reason, we investigated the effect of iron (II) chloride and iron (II) sulfate supplementation, which have higher absorption (*Harrington et al., 2011*) than iron (II) fumarate, on geNOps. Although all these iron supplements contain ferrous iron, $FeCl_2$ and $FeSO_4$ are found in hydrated form, so their solubility in water is higher than fumarate. The result of this study showed that both $FeCl_2$ and $FeSO_4$ had the same effect in geNOps with iron (II) fumarate without the need for extra mechanical mixing step (Figure 5.3).

Then, to investigate which is more stable between $FeCl_2$ and $FeSO_4$, we compared iron solutions stored at 4 °C for a day or a week with freshly prepared solutions on the day of the experiment. We also used fumarate as a control in this experiment. This result showed us that While the $FeCl_2$ and $FeSO_4$ solution prepared the day before gave similar responses to the freshly prepared ones, $FeSO_4$ prepared 1 week ago not only gave the same response as the fresh one but also showed that it was more stable than $FeCl_2$. Thus, all subsequent studies were continued with $FeSO_4$ (Figure 5.4). These results were obtained thanks to $FeSO_4$ is a water-soluble compound and is more stable in neutral pH conditions than iron compounds. In a study, it was observed that temperature change increased ferrous iron oxidation in bacteria grown in bioreactors (*Breed et al., 1999*).

It is possible for ferrous iron to be oxidized by gaining electrons in some situations, especially in the presence of oxygen (*Stumm et al., 1961*). This prevents the absorption of iron into the cell and prevents it from continuing its functions (*Ems et al., 2021*). Various reducing agents are also used in many in vitro studies to prevent oxidation of

iron. geNOps have been used as a Vitamin C reducing agent since the first time they were discovered because both the cell culture oxygen conditions and the physiological buffer used had a significant effect on iron oxidation (*Eroglu et al., 2016*). Both reduced glutathione (comprising glutamine, cysteine, and glycine) and cysteine are two important reducing agents in the reduction and absorption of iron (*Layrisse et al., 1984*). The cell culture media contains an amount of L-cysteine without any effect on iron oxidation. We used D-cysteine as a reducing agent in our study because it does not impair the functions in the cell. Our study showed that Vitamin C is more active in reducing iron than other reducing agents (Figure 5.5).

We investigated the effect of different cell culture media containing ferric and/or ferrous iron on geNOps functionality. And as a result, not only short-term treatment but also long-term treatment, we showed that for the reasons, cell culture media containing a less amount iron is insufficient for cells, adding Vitamin C is successful in reducing iron to some extent but not sufficient, only $FeSO_4$ is not stable due to both the physiological buffer and the cell culture oxygen, and acute $FeSO_4$ and Vitamin C supplementation is necessary for full function of geNOps (Figure 5.9–5.10). Most of the proteins in the cell perform their functions through metals (*Maret, 2010*). Iron is also one of the most important metals required for proteins (*Frieden, 1974*). The amount of both ferrous and/or ferric iron in cell culture media used for cells grown and studied under cell culture conditions is much lower than the amount found in normal physiological conditions (*Ganz & Nemeth, 2011*). Today, the amount of iron in DMEM used in cell culture is only 0.25 µM ferric nitrate, which is well below the physiological amount of iron required for the cell (*Spasojevic, 2016*). Since the same DMEM does not contain Vitamin C, which has a role in the reduction of iron and is an important cell supplement, it is expected event that iron is not reduced. Serum added to the cell culture medium contains varying amounts of iron and Vitamin C, but this is not sufficient (*Spasojevic, 2016*). This may cause the amount of iron required for biochemical reactions in the cell not to be achieved *in vitro* studies and the effects observed *in vivo* cannot be observed. In this study, we consider insufficient iron content in cell culture media as an important factor in the failure of other metalloproteins, like geNOps, that use iron as a cofactor.

We decided to develop a media by taking the amount of iron and Vitamin C in the cell

culture as a single factor based on the data shown in the previous experiment. We have let HEK293T cells grow for a long time with media containing $FeSO_4$ or Vitamin C prepared at certain concentrations. However, we have observed that a high concentration of iron and Vitamin C caused the morphological change of cells and their death in long-term treatment. Cell deaths were observed more quickly in cells treated with only Vitamin C. In obtaining these results, we think that the oxygen level of the cell culture is a pioneer in initiating the Fenton reactions, which can lead to the apoptosis of the cell by ferrous iron and converting Vitamin C ascorbate radicals (*Dixon & Stockwell, 2014*). Moreover, long-term incubation of Vitamin C at supraphysiological concentrations in cell culture conditions with high oxygen levels has been reported to be toxic to cells (*Zhitkovich, 2021*). In addition to this, it has been emphasized that high amounts of Vitamin C cause undesirable biological effects in human studies (*Podmore et al., 1998; Duarte & Lunec, 2005*) and the necessity of determining the optimum Vitamin C depending on the cell line (*Zhitkovich, 2021*). At the end of long-term treatment, we determined 16 mg/L $FeSO_4$ and 8 mg/L Vitamin C as the highest stable concentrations and showed that these concentrations were not effective on geNOps (Figure 5.11).

Then, we investigated the effect on geNOps by combining 16 mg/L $FeSO_4$ and 8 mg/L Vitamin C obtained from long-term treatment. We showed that this combination doesn't work either and even requires an acute treatment to work (Figure 5.12). The amount of Vitamin C used in this combination may not have reduced $FeSO_4$.

FeRhoNox-1, which is a turn-on fluorescent probe for labile ferrous iron in the cell, showed parallel results to the geNOps responses taken under the same conditions (Figure 5.6). The staining of the cells treated under different conditions showed us a certain intensity with FeRhoNox-1 under control conditions. In the article explaining the working principle of the probe, a weak fluorescent signal was observed in cells under control conditions (*Hirayama et al., 2013*). This supports the accuracy of our study. As a result of treatment with only Vitamin C, the observed signal increased, although not significantly. Here, some of the iron in the cell culture media may have been reduced with the help of Vitamin C which is an important reducing agent in the uptake of ferrous iron into the cell. In addition to increased signals, aggregation was also observed in cells treated with only $FeSO_4$. In the cells treated with Vitamin C and $FeSO_4$, we observed a homogeneous distribution of iron with increasing intensity. The change in intensity

observed in FeRhoNox-1 due to the increase in iron content is directly proportional to the change in signal observed in geNOps under the same conditions. Z-stacks taken with the aid of a high-resolution confocal microscope under the same conditions showed that the iron deposition was more on the cell surface (Figure 5.7). In the control group, the fluorescence intensity, which decreased as the cell was penetrated deeper, increased deeper in the cell in Vitamin C treatment. In addition, only treatment with $FeSO_4$ showed aggregation. We think that this may be due to the iron precipitating after a certain period in the physiological buffer we mentioned before because studies showing the precipitation of ferrous iron at high pH values support this finding (*Hove et al., 2008*). $FeSO_4$/Vitamin C treatment showed higher fluorescence intensity deeper in the cell. This shows that together with the reducing agent, iron supplementation can reach deeper into the cell. In addition, it is known that FeRhoNox-1 is localized to the Golgi and ER, but they are thought to be effective in detecting free ferrous iron in the cytoplasm (*Hirayama et al., 2013*). FerhoNox-1 accumulated on the surface maybe it binds iron there we don't know and localized undefinable intracellular structures. But still, the distribution of iron in the cell is still unclear.

To observe the intracellular distribution and accumulation of iron in addition to FeRhoNox-1 was Perls/DAB. Post-experimental images taken with 40X objective showed no difference between control and only Vitamin C-treated cells, while significant accumulations were observed in cells treated with only $FeSO_4$ and $FeSO_4$/Vitamin C. In the images taken at 100X to observe the distribution of these aggregations, it was determined that the accumulation observed only in the cells treated with $FeSO_4$ was extracellular, whereas in $FeSO_4$/Vitamin C there was no extracellular accumulation (Figure 5.8).

We could not determine what the required iron distribution should be with the different staining techniques. For this reason, we developed an optimized iron (II) loading procedure, which is sufficient for the functionality of geNOps and to prevent unwanted redox reactions later. For this, we observed the functionality of geNOps by creating the experimental conditions with the help of Taguchi, considering 3 parameters (concentration of $FeSO_4$ and Vitamin C and incubation time). The results of the

experimental conditions determined by Taguchi showed that incubation of geNOps with 300 µM $FeSO_4$ + 500 µM Vitamin C for 15 minutes has provided the same responses as the previously used standard solution (Figure 5.13). We have continued with these concentrations as they provide the same conditions with fewer concentrations (Figure 5.14). The cell viability in different treatment conditions did not change (Figure 5.15), and we have decided to treat the cells with the new optimized iron (II) solution for geNOps functionality.

The next step was to test this newly optimized iron solution in endothelial cells. Since the transfection efficiency of EA. hy926 cells are low, we have created EA. hy926 cells stably expressing O-geNOp-NES with the help of virus infection. The conversion of superoxide produced after mitochondrial respiration to hydrogen peroxides causes basal ROS to be contained within the cell. However, in excess iron conditions, the reaction of these H_2O_2 with the iron causes the formation of hydroxyl radicals, which irreversibly impair cellular functions. Also under this condition, since hydrogen peroxide formed would react with iron, a decrease in basal H_2O_2 would be expected in the presence of excess iron. For this reason, it is of great importance to providing an appropriate iron balance for the metalloproteins in the cell. We observed that the optimized solution used in the experiments is effective in the measurement of endogenously NO (Figure 5.16). In addition, the supplemented iron solution did not cause the formation of reactive oxygen species in different intracellular locations (Figure 5.17). No significant change was observed in the H_2O_2 basal level in HEK293T cells either. This draws attention to the presence of non-toxic iron concentrations that will enable the metalloproteins to perform their own functions under cell culture conditions with high oxygen levels.

In this study, it has been proven that geNOps is a reporter that can represent metalloproteins in the cell. Attention was drawn to the iron deficiency of the media used for cultured cells and the necessity of short-term reducing agent-supported iron supplements was emphasized. Optimization of the iron solution suitable for these conditions influenced the activation of the metalloprotein without causing ROS.

7. CONCLUSION

In this study, we modeled the ferrous iron (Fe^{2+}) deficiency problem experienced by iron-dependent metalloproteins under cell culture conditions by using geNOps, which is one of the important probes in living cells and contains iron-dependent metalloprotein in its structure. The effect of deficiency of ferrous iron, which cannot be supplemented with cell culture media, on metalloproteins has been indirectly demonstrated. Our study is the first step in emphasizing this problem experienced by other metalloproteins in the cell and is suitable for further development.

8. BIBLIOGRAPHY

Arai, S. (2019). The ABC Guide to Fluorescent Toolsets for the Development of Future Biomaterials. *Frontiers in bioengineering and biotechnology*, *7*, 5.

Aslamkhan, A. G., Aslamkhan, A., & Ahearn, G. A. (2002). Preparation of metal ion buffers for biological experimentation: a methods approach with emphasis on iron and zinc. *Journal of experimental zoology*, *292*(6), 507-522.

Azqueta, A., Costa, S., Lorenzo, Y., Bastani, N. E., & Collins, A. R. (2013). Vitamin C in cultured human (HeLa) cells: lack of effect on DNA protection and repair. *Nutrients*, *5*(4), 1200-1217.

Bertini, I., Ciurli, S., & Luchinat, C. (1995). The electronic structure of FeS centers in proteins and models a contribution to the understanding of their electron transfer properties. *Iron-Sulfur Proteins Perovskites*, 1-53.

Breed, A. W., Dempers, C. J. N., Searby, G. E., Gardner, M. N., Rawlings, D. E., & Hansford, G. S. (1999). The effect of temperature on the continuous ferrous-iron oxidation kinetics of a predominantly Leptospirillum ferrooxidans culture. *Biotechnology and bioengineering*, *65*(1), 44-53.

Breuer, W., Epsztejn, S., & Cabantchik, Z. I. (1995). Iron Acquired from Transferrin by K562 Cells Is Delivered into a Cytoplasmic Pool of Chelatable Iron (II)(∗). *Journal of Biological Chemistry*, *270*(41), 24209-24215.

Breuer, W. I. L. L. I. A. M., Epsztejn, S. I. L. V. I. N. A., Millgram, P. N. I. N. A., & Cabantchik, I. Z. (1995). Transport of iron and other transition metals into cells as revealed by a fluorescent probe. *American Journal of Physiology-Cell Physiology*, *268*(6), C1354-C1361.

Bush, M., Ghosh, T., Tucker, N., Zhang, X., & Dixon, R. (2011). Transcriptional regulation by the dedicated nitric oxide sensor, NorR: a route towards NO detoxification. *Biochemical Society Transactions*, *39*(1), 289-293

Bush, M., Ghosh, T., Sawicka, M., Moal, I. H., Bates, P. A., Dixon, R., & Zhang, X. (2015). The structural basis for enhancer-dependent assembly and activation of the AAA transcriptional activator NorR. *Molecular microbiology*, *95*(1), 17-30.

Carpenter, C. E., & Ward, R. E. (2017). Iron determination by Ferrozine method. In *Food Analysis Laboratory Manual* (pp. 157-159). Springer, Cham.

Charoensin, S., Eroglu, E., Opelt, M., Bischof, H., Madreiter-Sokolowski, C. T., Kirsch, A., ... & Malli, R. (2017). Intact mitochondrial Ca2+ uniport is essential for agonist-induced activation of endothelial nitric oxide synthase (eNOS). *Free Radical Biology and Medicine*, *102*, 248-259.

Chen, Q., Espey, M. G., Krishna, M. C., Mitchell, J. B., Corpe, C. P., Buettner, G. R., ... & Levine, M. (2005). Pharmacologic ascorbic acid concentrations selectively kill cancer cells: action as a pro-drug to deliver hydrogen peroxide to tissues. *Proceedings of the National Academy of Sciences*, *102*(38), 13604-13609.

Chudakov, D. M., Matz, M. V., Lukyanov, S., & Lukyanov, K. A. (2010). Fluorescent proteins and their applications in imaging living cells and tissues. *Physiological reviews*, *90*(3), 1103-1163.

D'Autréaux, B., Tucker, N. P., Dixon, R., & Spiro, S. (2005). A non-haem iron centre in the transcription factor NorR senses nitric oxide. *Nature*, *437*(7059), 769-772.

Depaoli, M. R., Bischof, H., Eroglu, E., Burgstaller, S., Ramadani-Muja, J., Rauter, T., ... & Malli, R. (2019). Live cell imaging of signaling and metabolic activities. *Pharmacology & therapeutics*, *202*, 98-119.

Dixon, S. J., & Stockwell, B. R. (2014). The role of iron and reactive oxygen species in cell death. *Nature chemical biology*, *10*(1), 9-17.

Duarte, T. L., & Lunec, J. (2005). Review part of the series: From dietary antioxidants to regulators in cellular signalling and gene expression review: When is an antioxidant not an antioxidant? A review of novel actions and reactions of vitamin C. *Free radical research*, *39*(7), 671-686.

Ems, T., & Huecker, M. R. (2021). Biochemistry, iron absorption. *StatPearls [internet]*.

Eroglu, E., Gottschalk, B., Charoensin, S., Blass, S., Bischof, H., Rost, R., ... & Malli, R. (2016). Development of novel FP-based probes for live-cell imaging of nitric oxide dynamics. *Nature communications*, *7*(1), 1-11.

Eroglu, E., Hallström, S., Bischof, H., Opelt, M., Schmidt, K., Mayer, B., ... & Malli, R. (2017). Real-time visualization of distinct nitric oxide generation of nitric oxide synthase isoforms in single cells. *Nitric Oxide*, *70*, 59-67.

Eroglu, E., Charoensin, S., Bischof, H., Ramadani, J., Gottschalk, B., Depaoli, M. R., ... & Malli, R. (2018). Genetic biosensors for imaging nitric oxide in single cells. *Free Radical Biology and Medicine*, *128*, 50-58.

Fedeles, B. I., Singh, V., Delaney, J. C., Li, D., & Essigmann, J. M. (2015). The AlkB family of Fe (II)/α-ketoglutarate-dependent dioxygenases: repairing nucleic acid alkylation damage and beyond. *Journal of Biological Chemistry*, *290*(34), 20734-20742.

Fish, W. W. (1988). Rapid colorimetric micromethod for the quantitation of complexed iron in biological samples in Methods in Enzymology (Riordan, JF and Vallee, BL, eds.)

Vol. 158A.

Franken, L. E., Grünewald, K., Boekema, E. J., & Stuart, M. C. (2020). A Technical Introduction to Transmission Electron Microscopy for Soft-Matter: Imaging, Possibilities, Choices, and Technical Developments. *Small*, *16*(14), 1906198.

Frieden, E. (1976). Copper and iron metalloproteins. *Trends in Biochemical Sciences*, *1*(4), 273-274.

Ganz, T., & Nemeth, E. (2011). Hepcidin and disorders of iron metabolism. *Annual review of medicine*, *62*, 347-360.

Galaris, D., Barbouti, A., & Pantopoulos, K. (2019). Iron homeostasis and oxidative stress: An intimate relationship. *Biochimica et Biophysica Acta (BBA)-Molecular Cell Research*, *1866*(12), 118535.

Gao, T., & O'Brian, M. R. (2005). Iron-dependent cytochrome c 1 expression is mediated by the status of heme in Bradyrhizobium japonicum. *Journal of bacteriology*, *187*(15), 5084-5089.

Ganz, T., & Nemeth, E. (2011). Hepcidin and disorders of iron metabolism. *Annual review of medicine*, *62*, 347-360.

García-Casal, M. N., & Layrisse, M. (2001). The effect of change in pH on the solubility 01 iron bis-glycinate chelate and other iron compounds. *Archivos latinoamericanos de nutricion*, *51*(1), 35-36.

Greenwald, E. C., Mehta, S., & Zhang, J. (2018). Genetically encoded fluorescent biosensors illuminate the spatiotemporal regulation of signaling networks. *Chemical reviews*, *118*(24), 11707-11794.

Harrington, M., Hotz, C., Zeder, C., Polvo, G. O., Villalpando, S., Zimmermann, M. B., ... & Hurrell, R. F. (2011). A comparison of the bioavailability of ferrous fumarate and ferrous sulfate in non-anemic Mexican women and children consuming a sweetened maize and milk drink. *European journal of clinical nutrition*, *65*(1), 20-25.

Hirayama, T., Okuda, K., & Nagasawa, H. (2013). A highly selective turn-on fluorescent probe for iron (II) to visualize labile iron in living cells. *Chemical science*, *4*(3), 1250-1256.

Hirayama, T., & Nagasawa, H. (2017). Chemical tools for detecting Fe ions. *Journal of clinical biochemistry and nutrition*, *60*(1), 39-48.

Hoppert, M. (2011). Metalloenzymes. In *Encyclopedia of Geobiology*.

Hove, M., van Hille, R. P., & Lewis, A. E. (2008). Mechanisms of formation of iron precipitates from ferrous solutions at high and low pH. *Chemical Engineering Science*, *63*(6), 1626-1635.

J., Nikolić, L. B., Nikolić, V. D., Stanković, M. Z., Cakić, M. D., Ilić, D. P., ... & Ristić, I. S. (2012). The synthesis and characterization of iron (II) fumarate and its inclusion complexes with cyclodextrins. *Advanced technologies*, *1*(1), 7-15.

Khan, M. T., & Martell, A. E. (1967). Metal ion and metal chelate catalyzed oxidation of ascorbic acid by molecular oxygen. I. Cupric and ferric ion catalyzed oxidation. *Journal of the American Chemical Society*, *89*(16), 4176-4185.

Kakuta, K., Orino, K., Yamamoto, S., & Watanabe, K. (1997). High levels of ferritin and its iron in fetal bovine serum. *Comparative Biochemistry and Physiology Part A: Physiology*, *118*(1), 165-169.

Kawabata, H. (2019). Transferrin and transferrin receptors update. *Free Radical Biology and Medicine*, *133*, 46-54.

Knutson, M. D. (2019). Non-transferrin-bound iron transporters. *Free Radical Biology and Medicine*, *133*, 101-111.

Kim, H., Ju, J., Lee, H. N., Chun, H., & Seong, J. (2021). Genetically Encoded Biosensors Based on Fluorescent Proteins. *Sensors*, *21*(3), 795.

Kumfu, S., Chattipakorn, S. C., Fucharoen, S., & Chattipakorn, N. (2016). Dual T-type and L-type calcium channel blocker exerts beneficial effects in attenuating cardiovascular dysfunction in iron-overloaded thalassaemic mice. *Experimental physiology*, *101*(4), 521-539.

Lane, D. J., Bae, D. H., Merlot, A. M., Sahni, S., & Richardson, D. R. (2015). Duodenal cytochrome b (DCYTB) in iron metabolism: an update on function and regulation. *Nutrients*, *7*(4), 2274-2296.

Layrisse, M., Martínez-Torres, C., Leets, I., Taylor, P., & Ramírez, J. (1984). Effect of histidine, cysteine, glutathione or beef on iron absorption in humans. *The Journal of nutrition*, *114*(1), 217-223.

Li, J., Cao, F., Yin, H. L., Huang, Z. J., Lin, Z. T., Mao, N., ... & Wang, G. (2020). Ferroptosis: past, present and future. *Cell death & disease*, *11*(2), 1-13.

Lopin, K. V., Gray, I. P., Obejero-Paz, C. A., Thevenod, F., & Jones, S. W. (2012). Fe2+ block and permeation of CaV3. 1 (α1G) T-type calcium channels: Candidate mechanism for non–transferrin-mediated Fe2+ influx. *Molecular pharmacology*, *82*(6), 1194-1204.

Lőrincz, T., Holczer, M., Kapuy, O., & Szarka, A. (2019). The interrelationship of pharmacologic ascorbate induced cell death and ferroptosis. *Pathology & Oncology Research*, *25*(2), 669-679.

Malatesta, M. (2021). Transmission Electron Microscopy as a Powerful Tool to Investigate the Interaction of Nanoparticles with Subcellular Structures. *International Journal of Molecular Sciences*, *22*(23), 12789.

Maret, W. (2010). Metalloproteomics, metalloproteomes, and the annotation of metalloproteins. *Metallomics*, *2*(2), 117-125.

Meguro, R., Asano, Y., Odagiri, S., Li, C., Iwatsuki, H., & Shoumura, K. (2007). Nonheme-iron histochemistry for light and electron microscopy: a historical, theoretical and technical review. *Archives of histology and cytology*, *70*(1), 1-19.

Merkofer, M., Kissner, R., Hider, R. C., Brunk, U. T., & Koppenol, W. H. (2006). Fenton chemistry and iron chelation under physiologically relevant conditions: electrochemistry and kinetics. *Chemical research in toxicology*, *19*(10), 1263-1269.

Meyer, S., López-Serrano, A., Mitze, H., Jakubowski, N., & Schwerdtle, T. (2018). Single-cell analysis by ICP-MS/MS as a fast tool for cellular bioavailability studies of arsenite. *Metallomics*, *10*(1), 73-76.

Michels, A. J., & Frei, B. (2013). Myths, artifacts, and fatal flaws: identifying limitations and opportunities in vitamin C research. *Nutrients*, *5*(12), 5161-5192.

Mojić, M., Pristov, J. B., Maksimović-Ivanić, D., Jones, D. R., Stanić, M., Mijatović, S., & Spasojević, I. (2014). Extracellular iron diminishes anticancer effects of vitamin C: an in vitro study. *Scientific reports*, *4*(1), 1-8.

Nakamura, T., Naguro, I., & Ichijo, H. (2019). Iron homeostasis and iron-regulated ROS in cell death, senescence and human diseases. *Biochimica et Biophysica Acta (BBA)-General Subjects*, *1863*(9), 1398-1409.

Nguyen-Legros, J., Bizot, J., Bolesse, M., & Pulicani, J. P. (1980). " Diaminobenzidine black" as a new histochemical demonstration of exogenous iron (author's transl). *Histochemistry*, *66*(3), 239-244.

Niwa, M., Hirayama, T., Okuda, K., & Nagasawa, H. (2014). A new class of high-contrast Fe (II) selective fluorescent probes based on spirocyclized scaffolds for visualization of intracellular labile iron delivered by transferrin. *Organic & biomolecular chemistry*, *12*(34), 6590-6597.

Opelt, M., Eroglu, E., Waldeck-Weiermair, M., Russwurm, M., Koesling, D., Malli, R., ... & Mayer, B. (2016). Formation of nitric oxide by aldehyde dehydrogenase-2 is necessary and sufficient for vascular bioactivation of nitroglycerin. *Journal of Biological Chemistry*, *291*(46), 24076-24084.

Parrow, N. L., Leshin, J. A., & Levine, M. (2013). Parenteral ascorbate as a cancer therapeutic: a reassessment based on pharmacokinetics. *Antioxidants & redox signaling*, *19*(17), 2141-2156.

Podmore, I. D., Griffiths, H. R., Herbert, K. E., Mistry, N., Mistry, P., & Lunec, J. (1998). Vitamin C exhibits pro-oxidant properties. *Nature*, *392*(6676), 559-559.

Ren, W., & Ai, H. W. (2013). Genetically encoded fluorescent redox probes. *Sensors*, *13*(11), 15422-15433.

Riemer, J., Hoepken, H. H., Czerwinska, H., Robinson, S. R., & Dringen, R. (2004). Colorimetric ferrozine-based assay for the quantitation of iron in cultured cells. *Analytical biochemistry*, *331*(2), 370-375.

Ring, H., Gao, Z., Klein, N. D., Garwood, M., Bischof, J. C., & Haynes, C. L. (2018). Ferrozine assay for simple and cheap iron analysis of silica-coated iron oxide nanoparticles.

Roschzttardtz, H., Conéjéro, G., Curie, C., & Mari, S. (2010). Straightforward histochemical staining of Fe by the adaptation of an old-school technique: identification of the endodermal vacuole as the site of Fe storage in Arabidopsis embryos. *Plant signaling & behavior*, *5*(1), 56-57.

Secilmis, M., Altun, H. Y., Pilic, J., Erdogan, Y. C., Cokluk, Z., Ata, B. N., ... & Eroglu, E. (2021). A co-culture-based multiparametric imaging technique to dissect local H2O2 signals with targeted HyPer7. *Biosensors*, *11*(9), 338.

Sharp, P., & Srai, S. K. (2007). Molecular mechanisms involved in intestinal iron absorption. *World journal of gastroenterology: WJG*, *13*(35), 4716.

Shayeghi, M., Latunde-Dada, G. O., Oakhill, J. S., Laftah, A. H., Takeuchi, K., Halliday, N., ... & McKie, A. T. (2005). Identification of an intestinal heme transporter. *Cell*, *122*(5), 789-801.

Sheehan, D. C., & Hrapchak, B. B. (1980). Theory and practice of histotechnology 2nd edition. *Edited by: Mosby CV. St. Louis, MO: The CV Mosby Company*.

Sherman, H. G., Jovanovic, C., Stolnik, S., Baronian, K., Downard, A. J., & Rawson, F. J. (2018). New perspectives on iron uptake in eukaryotes. *Frontiers in molecular biosciences*, *5*, 97.

Spasojević, I. (2016). What if cell culture media do not mimic in vivo redox settings?. *Redox Report*, *21*(3), 127-129.

Spiro, S. (2007). Regulators of bacterial responses to nitric oxide. *FEMS microbiology reviews*, *31*(2), 193-211.

Stookey, L. L. (1970). Ferrozine---a new spectrophotometric reagent for iron. *Analytical chemistry*, *42*(7), 779-781.

Stumm, W., & Lee, G. F. (1961). Oxygenation of ferrous iron. *Industrial & Engineering Chemistry*, *53*(2), 143-146.

Tenopoulou, M., Kurz, T., Doulias, P. T., Galaris, D., & Brunk, U. T. (2007). Does the calcein-AM method assay the total cellular ‘labile iron pool’or only a fraction of it?. *Biochemical Journal*, *403*(2), 261-266.

Timoshnikov, V. A., Kobzeva, T. V., Polyakov, N. E., & Kontoghiorghes, G. J. (2020). Redox interactions of vitamin C and iron: Inhibition of the pro-oxidant activity by deferiprone. *International Journal of Molecular Sciences*, *21*(11), 3967.

Waldvogel-Abramowski, S., Waeber, G., Gassner, C., Buser, A., Frey, B. M., Favrat, B., & Tissot, J. D. (2014). Physiology of iron metabolism. *Transfusion Medicine and Hemotherapy*, *41*(3), 213-221.

Wang, J., & Pantopoulos, K. (2011). Regulation of cellular iron metabolism. *Biochemical Journal*, *434*(3), 365-381.

Wilschefski, S. C., & Baxter, M. R. (2019). Inductively coupled plasma mass spectrometry: introduction to analytical aspects. *The Clinical Biochemist Reviews*, *40*(3), 115.

Verschoor, M. J., & Molot, L. A. (2013). A comparison of three colorimetric methods of ferrous and total reactive iron measurement in freshwaters. *Limnology and Oceanography: Methods*, *11*(3), 113-125.

Yao, X., & Garland, C. J. (2005). Recent developments in vascular endothelial cell transient receptor potential channels. *Circulation research*, *97*(9), 853-863.

Zhitkovich, A. (2020). Nuclear and cytoplasmic functions of vitamin C. *Chemical research in toxicology*, *33*(10), 2515-2526.

Zhitkovich, A. (2021). Ascorbate: antioxidant and biochemical activities and their importance for in vitro models. *Archives of Toxicology*, 1-9.

9. APPENDICES

9.1. Appendix A: Chemicals

Chemicals	Manufacturing Company
Adenosine Triphosphate (ATP)	Sigma Aldrich, USA
Advanced DMEM	Gibco, USA
Ampicillin	Sigma Aldrich, USA
Calcium chloride ($CaCl_2$)	neoFroxx, Germany
D-Cysteine	ChemCruz, Germany
Dimethyl sulfoxide (DMSO)	PAN-Biotech, Germany
D (+) Glucose	neoFroxx, Germany
Dulbecco's Modified Eagle Medium	PAN-Biotech, Germany
Essential amino acids	PAN-Biotech, Germany
Ethanol	Merck, Germany
FeRhoNox-1	Goryo Chemical, Japan
Ferrozine	Sigma Aldrich, USA
Fetal Bovine Serum (FBS)	PAN-Biotech, USA
Glycerol	neoFroxx, Germany
Ham's F12 Medium	PAN-Biotech, Germany
Ham's F12K Medium	Gibco, USA
HAT supplement	LGC Standards, Turkey
HEPES	PAN-Biotech, Germany
Hoechst 33342	HelloBio, UK
Hydrochloric acid (HCl)	Merck, Germany
Hydrogen peroxide (H_2O_2)	neoFroxx, Germany
Iron (II) chloride ($FeCl_2$)	Iron (II) sulfate ($FeSO_4$)
Iron (II) fumarate (C_4H_2FeO4)	Isopropanol

L-ascorbic acid	Merck, Germany
L-Glutathione	Merck, Germany
Liquid Broth	neoFroxx, Germany
Magnesium chloride ($MgCl_2$)	PAN-Biotech, Germany
MEM vitamins	Sigma Aldrich, USA
Monopotassium phosphate (KH_2PO_4)	neoFroxx, Germany
NOC-7	PAN-Biotech, Germany
Normocin	neoFroxx, Germany
Penicillin/Streptomycin	Santa Cruz Biotechnology, USA
Phosphate Buffered Saline	Invivogen, France
PolyJet	PAN-Biotech, Germany
Potassium Chloride (KCl)	PAN-Biotech, Germany
Propidium Iodide (PI)	SignaGen Laboratories, USA
Serum-Free Phenol Red Free DMEM	neoFroxx, Germany
Sodium bicarbonate ($NaHCO_3$)	Invitrogen, USA
Sodium chloride (NaCl)	PAN-Biotech, Germany
Sodium hydroxide (NaOH)	neoFroxx, Germany
Sodium pyruvate ($C_3H_3NaO_3$)	neoFroxx, Germany
Trypsin-EDTA	Sigma Aldrich, USA
Sigma Aldrich, USA	PAN-Biotech, Germany
Alfa Aesar, USA	PAN-Biotech, Germany

9.2. Appendix B: Equipment

Equipment	Manufacturing Company
Axio Observer. Z17	Zeiss, Germany
Axia Vert.A1	Zeiss, Germany
Axiocam 503 mono	Zeiss, Germany
Balance	Ohaus, USA
Biosafety Hood	Nuve, Turkey
CO2 chamber	Nuve, Turkey
Colibri 2 Light Source	Zeiss, Germany
Colibri 7 Light Source	Zeiss, Germany
Glass coverslips	Asistent, Germany
Heal block	Eppendorf, Germany
Hemocytometer	Isolab, Germany
Laser Scanning Confocal Microscope 800	Zeiss, Germany
Nanodrop	Thermo Scientific, USA
Perfusion Chamber	NGFI, Austria
pHmeter	Ohaus, USA
Plan-Apochromat 40x/1.4 Oil	Zeiss, Germany
Plan-Apochromat 20x/0.8 M27	Zeiss, Germany
Shaking incubator	New Brünswick, USA
Tabletop centrifuge	Eppendorf, Germany
Tabletop centrifuge	Beckman-Coulter, USA
ThermoCycler	BioRad, USA
Waterbath	Nuve, Turkey

9.3. Appendix C: Molecular Biology Kits & Enzymes

Kit & Enzymes	Manufacturing Company
Midiprep DNA Isolation	Qiagen, Germany
BamHI	NEB, USA
SalI	NEB, USA